Modelling and Simulation of Three Wheeler Electric Vehicle Propelled by Permanent Magnet Direct Current Motor

Abdissa Regassa Negash

A Thesis Submitted to

The Department of Mechanical Engineering

School of Mechanical, Chemical and Materials Engineering

Presented in Partial Fulfilment of the Requirement for the Degree of Master's

In Automotive Engineering

Office of Graduate Studies

Adama Science and Technology University

January, 2024

Adama, Ethiopia

Modelling and Simulation of Three Wheeler Electric Vehicle Propelled by Permanent Magnet Direct Current Motor

Abdissa Regassa Negash

Advisor: Dr. Alemayehu Wakjira

A Thesis Submitted to

The Department of Mechanical Engineering

School of Mechanical, Chemical and Materials Engineering

Presented in Partial Fulfilment of the Requirement for Degree of Master's

In Automotive Engineering

Office of Graduate Studies

Adama Science and Technology University

January, 2024

Adama, Ethiopia

DECLARATION

I hereby certify that the work presented in the thesis entitled "**Modelling and Simulation of Three Wheeler Electric Vehicle Propelled by Permanent Magnet DC Motor** " submitted in partial fulfilment of the requirements for the award of the degree of Masters of Science in Automotive Engineering, is an authentic record of my own work completed from October 2022 to January 2024 under the guidance of Dr. Alemayehu Wakjira, Department of Mechanical Engineering.

Abdissa Regassa Negash	__________________	______________
Name of student	Signature	Date

RECOMMENDATION

I, the thesis advisor, hereby certify that I have read the revised version of the thesis entitled "**Modelling and Simulation of Three Wheeler Electric Vehicle Propelled by Permanent Magnet DC Motor**" prepared under my supervision by Abdissa Regassa and submitted in partial fulfilment of the requirements for Masters of Science in automotive engineering. As a result, I recommend the submission of the revised version of the thesis to the department in accordance with the applicable procedure.

Dr. Alemayehu Wakjira (Ph.D)	_______________	______________
Major Advisor	Signature	Date

APPROVAL SHEET

I, the advisor of the thesis entitled "**Modelling and Simulation of Three Wheeler Electric Vehicle Propelled by Permanent Magnet DC Motor**" and developed by Abdissa Regassa, hereby certify that the recommendation and suggestions made by the board of examiners are appropriately incorporated into the final version of the thesis.

Dr. Alemayehu Wakjira (Ph.D) ______________________ __________________

Major Advisor Signature Date

We, the undersigned members of the Board of Examiners of the thesis by Abdissa Regassa have read and evaluated the thesis entitled "**Modelling and Simulation of Three Wheeler Electric Vehicle Propelled by Permanent Magnet DC Motor**" and examined the candidate during open defence. This is, therefore, to certify that the thesis is accepted for partial fulfilment of the requirement of the degree of Masters of Science in Automotive Engineering.

_______________________ ____________________ _________________

Chair Person Signature Date

Dr. Getachew Alemayehu (Ph.D) ____________________ _______________

Internal Examiner Signature Date

Dr. Bisirat Yoseph (Ph.D) ____________________ _______________

External Examiner Signature Date

Finally, approval and acceptance of the thesis is contingent upon submission of its final copy to the Office of Postgraduate Studies (OPGS) through the Department Graduate Council (DGC) and School Graduate Committee (SGC).

__________________________ ______________________ __________________

Department Head Signature Date

__________________________ ______________________ __________________

School Dean Signature Date

__________________________ ______________________ __________________

Office of Postgraduate Studies, Dean Signature Date

ACKNOWLEDGEMENT

I want to start by giving thanks to the Almighty God for all of his favours and gifts! The success of this thesis would not have been possible without the ongoing corrections and helpful criticism provided by my adviser, Dr. Alemayehu Wakjira (Ph.D). I would like to extend my sincere gratitude to him for his scientific and technical advice and support throughout this thesis. My MSc advisor, Dr. Alemayehu Wakjira (Ph.D), guided me throughout the entire thesis process, right down to title selection. I appreciate the support from all of the ASTU School of Mechanical, Chemical, and Materials Engineering staff in enabling me to enrol in this MSc. programme. I also want to express my gratitude to my cheerleaders Regassa, Tejitu, Kena, and Ayantu for their unending support and encouragement throughout my life. Last but not least, I want to express my gratitude to all of my friends and colleagues for their inspiration and contributions of time, money, and ideas.

TABLE OF CONTENTS

LIST OF TABLES

LIST OF FIGURES

ACRONYMS

AISI-------------------------------------American Iron and Steel Institute

BEV--------------------------------------Battery Electric Vehicle

BLDCM---------------------------------Brushless Direct Current Motor

CNG-------------------------------------Compressed Natural Gas

CAD-------------------------------------Computer Aided Drafting

DC---------------------------------------Direct Current

EV---------------------------------------Electric Vehicle

EMF-------------------------------------Electromagnetic Force

FCV-------------------------------------Fuel Cell Vehicle

FEA-------------------------------------Finite Element Analysis

FTP-------------------------------------Federal Test Procedure

GMC-----------------------------------Generic Model Control

GHG-----------------------------------Green House Gas

HEV------------------------------------Hybrid Electric Vehicle

LPG-------------------------------------Liquefied Petroleum Gas

PMDCM-------------------------------Permanent Magnet Direct Current Motor

PID--------------------------------------Proportional Integral Derivatives

PHV-------------------------------------Plug in Hybrid Vehicle

PMSM---------------------------------Permanent Magnet Synchronous Motor

SRM-----------------------------------Switched Reluctance Motor

SOC-------------------------------------State of Charge

ZEV-------------------------------------Zero Emission Vehicles

ABSTRACT

With the global trend in the electrification of transportation, *Ethiopia also has started to follow the same trend. Especially with the significant foreign currency flow due to fossil fuel importation and greenhouse gas effect a seriously alternatives of energy source must be considered. Within this scenario the potential for the need of electric vehicles immerging in the country. Previously many researchers done the research on the three wheeler electric vehicle but, they focus on one component parameters. That study didn't bring the needed performance of the vehicle on different drive roads. The major bottleneck for electric vehicles were the energy storing system and range covered. Considering the above challenges and limitations it was needed to model three wheeler electric vehicle to solve the problems related with the above mentioned issues. The goal of this thesis paper is to model and create a three-wheeled electric vehicle powered by a permanent magnet direct current motor. The usage of permanent magnet DC motors is increasing in the EV industry due to their affordability, the lack of a controller required for a set speed, cheaper and their high torque characteristics at full load, which make them suitable for traction applications. The thesis was completed using solidwork modelling, ansys analysis of the chassis, and simulation of the power train using Matlab/ Simulink. From the simulation it was observed that the battery loses 34% SOC after travelling for 66.5 km as drive with 65km/r reference speed drive cycle for 2400 seconds, however it still maintains a SOC of 66%. But, if the fully charged battery is used the range covered for single charged battery was about 195 km and the speed of the vehicle also improved to 66.84km/hr. The deformation resistant capacity of the modelled and analysed chassis frame also improve the performance of the vehicle. It was assessed how well the battery, motor, controller, chassis, and overall performance of the three-wheeled electric vehicle perform. In order to maximise the use of green energy, different simulation results from a Mat-lab and CAD modelling was implemented on three-wheeled electric vehicle as the study's ultimate final result.*

Keywords: *Chassis Frame, Electric Motor, Electric Vehicle, State of Charge.*

CHAPTER ONE

INTRODUCTION

1.1. Background

Our reliance on fossil fuels has expanded as a result of the widespread use of ICE automobiles. Because fossil fuel extraction is one of the primary causes of the greenhouse gas effect, it comes with a huge environmental cost. Currently, different forms of transport account for close to 14% of global greenhouse gas emissions; it is predicted that by 2030, that number would increase to 50%. Due to the high concentrations of carbon dioxide and other climatically hazardous pollutants, both the environment and humanity are in danger. Conventional vehicles now use cleaner fuels and petrol catalysts to lessen the effects of these pollutants. The greenhouse effect is mostly caused by carbon dioxide emissions, which haven't been greatly reduced by these measures (Garling, A., & Thogersen, 2001).

According to the aforementioned conclusions and other research estimates, a more ecologically friendly transportation system is necessary. The availability of other energy sources or modifications to fuel properties can reduce emissions and promote the use of alternative fuels in place of conventional petrol and diesel. Because of these concerns, hybrid and battery-powered electric vehicles must now be adopted and deployed. This idea only applies to electric vehicles that are completely powered by batteries composed of electricity.

Electric cars are propelled by one or more electric motors that run on rechargeable batteries. Because electric vehicles can rely on renewable energy sources, switching to them helps to ensure an independent, greener, and more secure energy future (2013) (Daziano, R. A., & Chiew, E.). Electric vehicles are sometimes referred to as the cars of the future since they are incredibly efficient, create no local pollution, are silent, and can be used for power regulation by the grid operator. Electric vehicles still have a number of serious issues that need to be resolved.

The three main problems are a short driving range, a long charging time, and a high price. The car's battery system is a common link between the three main issues. PMDC motors are contemporary energy-saving drives that are incredibly reliable, efficient, and affordable. They are especially well-liked in industrial applications like automotive, aerospace, industrial automation, etc. (W. Jaffe and T.J. Sokira, 2009).

The challenge of implementing the required control functions by a new generation of microcontrollers and state-of-the-art electronics to give the PMDC motor a more realistic appearance. Three-wheelers are lighter and cheaper to construct, but because of their less forgiving design, they are less appropriate for applications with subpar design. (P. Thirisakthimurugan and P. Dananjayan, 2007).

The current study's objective was to model and create a three-wheeled electric vehicle using a PMDC motor in order to protect the environment and conserve energy. The battery pack must be strong enough to withstand accelerations and decelerations and have enough energy to cover a specific number of kilometres. To anticipate the energy consumption of an electric automobile, a precise model of the vehicle is essential.

Due to the fact that existing batteries' capacity does not allow for unlimited driving range but instead necessitates extensive recharging times and a high initial purchase price, potential customers are concerned about technical issues including driving range, cost, and charging technique. The main problem is that, although it is not true in the long run, an electric car initially costs substantially more than a regular car.

Significant barriers to buying electric automobiles include their high purchase price, constrained driving range, lack of charging stations, and the length of the charging process. On the one hand, it is initially believed that electric cars waste time and money, but on the other hand, they provide affordable gasoline, electric motors with a longer lifespan than the internal combustion engines of conventional automobiles, and lower maintenance expenses. (Daziano, R. A., & Chiew, E., 2013).

Since an electric car has so many unique components, including a battery, electric motor, transmission, and power electronics, its model is highly complex. To prevent coming to the wrong conclusions, each component must be correctly modelled. Designing or rating each component can be difficult because one component's specs can affect another's power output. This increases the likelihood that the car will be overpriced or underperform because there is a chance that one component may receive an inaccurate grade.

Additionally, dedicated EV manufacturers have appeared everywhere. Because it required assessing customer preferences for a product that they are mainly unfamiliar with, forecasting future demand for electric vehicles was somewhat challenging.

As a result, the development of electric vehicles focused on informing consumers about EV technologies and products, as well as their perceptions of EV brand, price, range, charging, infrastructure, and cost of ownership, as well as how an EV might fit into the consumer's lifestyle given a variety of demographic factors. Block diagram and general features of the electric vehicles are simulated by (Sreejith R. et.al, 2016).

In order to lessen the pollution issue created by conventional petrol models, rickshaw businesses have recently introduced alternate models that use Liquefied petroleum gas (LPG) and compressed natural gas (CNG) are also acceptable fuels. The ideal method to modify the three-wheeled vehicle is to use a highly efficient motor drive and make renewable energy the primary power source (J.F. Gieras and Wing, 2009). Due to their modest top speeds and short travel distances, three-wheelers make an excellent candidate for electrification. The general features of every electric vehicles includes battery, motor, motor controllers and vehicle body (Sinha, R., and Bangia, S., 2021).

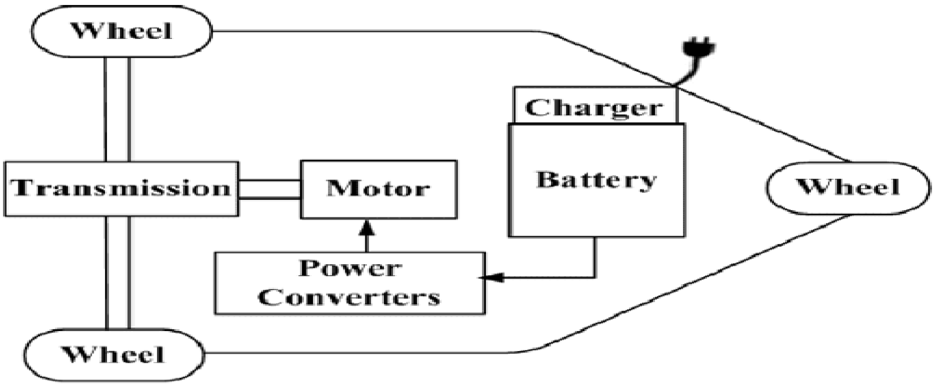

Figure 1. 1: Block Diagram for Three wheeler Electric vehicle *(Sreejith R. et. al, 2016)*

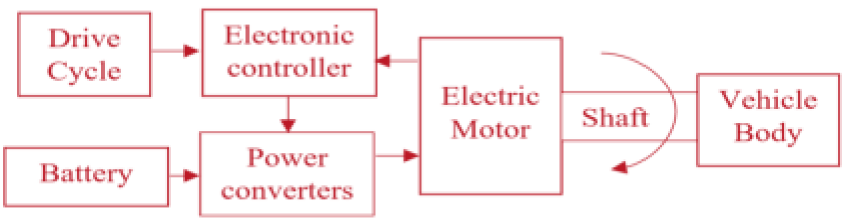

Figure 1. 2: General Features of Electric Vehicle (Sinha, R., and Bangia, S., 2021)

Figure 1.2 above depicts the general block diagram of an EV, which includes numerous controllers, an electric motor, a battery, power converters, and a vehicle body. All of these components need to work together for the car to run. For any electric vehicle's electric motor is a major component since the reliability of the motor is essential. The PMDC motor, often known as the DC motor, is the ideal electric motor for an electric vehicle due to its many benefits over synchronous motor and induction motor (J. Zhang, X. Lu, J. Xue, and B. Li, 2008).

Brushless DC motors are a type of synchronised motor. This illustrates that the stator and rotor's magnetic fields are generated at the same frequency. In contrast to a DC brushed motor, a PMDC motor has permanent magnets connected on the rotor. The border is frequently surrounded by four magnets. A stator is the component of a motor that contains electromagnets, often four of them.

The fundamental advantage of brushless motors is that they do not require the construction of a brush-commutation pair since the rotor performs as though it were made of permanent magnets, eliminating the requirement for rotor winding connections. Typically, this is where the phrase "brushless motors" originates. A speed controller was required for the brushless DC motor drive to regulate speed and provide quick braking.

Numerous techniques and algorithms for DC and brushless DC motor speed controllers have been proposed by researchers (A. A. R., 2013). Among them are PI, PID, fuzzy, and adaptive fuzzy. Brushless DC motor speeds are typically controlled by PID controllers. Due to its simple design and dependable functioning, PID controllers are widely used in a variety of industrial processes. PID controllers can manage both time and frequency responses when set up appropriately, but for complex systems, their performance tends to suffer. With the advent of fuzzy logic controllers, the performance of the controllers significantly changed. Fuzzy logic controllers are employed in a wide variety of industrial applications. When compared to PID controllers, the performance of this fuzzy logic controller is improved (A. A. R,, 2013).

1.2. Statement of the Problem

With the global trend in the electrification of transportation, Ethiopia also has started to follow the same trend. Especially with the significant foreign currency flow due to fossil fuel importation and greenhouse gas effect a seriously alternatives of energy source must be considered. Within this scenario the potential for the need of electric vehicles immerging in the country. The major bottleneck for electric vehicles was the range anxiety. Electric vehicle motor and battery usage is a significant factor that requires effective and appropriate control techniques for the improvement of vehicle performance. Different motor types are employed in the modelling of three-wheeler electric motors, but some of them have drawbacks compared to others.

1.3. Objectives

1.3.1. General Objectives

The general objective of this thesis work is to design, model, and simulate three wheeler electric vehicle propelled by permanent magnet DC motor using MATLAB Simulink, SolidWorks and ANSYS software.

1.3.2. Specific Objectives

These are the precise goals of this thesis project:

- To design and analysis of three wheeler electric vehicle chassis frame using SolidWorks and ANSYS software.
- To model the power train of three wheeler electric vehicle including necessary components.
- To simulate the state of charge of the battery for a chosen parameters of battery, motor, vehicle body and other components by using MATLAB Simulink modelling of battery.
- To simulate the range covered by the three wheeler electric vehicle for a single charged battery.

1.4. Motivation of the Study

The automotive industry is conducting research to increase vehicle efficiency as the global economy moves towards sustainable energy in response to climate change. Electric vehicles (EVs) are a solution to the crisis that the globe will soon be experiencing. However, the question that keeps coming up is how to extend the driving range of electric vehicles. The success of research of powerful energy sources like enchantment batteries, fuel cells, effective regenerative braking systems, etc. will determine the solution to this query. According to E. Bostanci, Z. Neuschl, and R. Plikat (2008), Regenerative braking enables the conversion of the vehicle's kinetic energy into electrical energy, which can then be stored in batteries and used to power the vehicle once more while it is being driven. By balancing energy in this way, regenerative braking can improve fuel economy while reducing pollutants that aggravate air pollution.

1.5. Limitation of the Study

The thesis is limited to the simulation of the system using the softwares Matlab/Simulink, solidworks, and ansys by demonstrating how the various system components interact with one another. This is because the implementation of a real system is challenging to procure the components for, along with the additional time and expense incurred in making the actual prototype implementation.

1.6. Significance of the Study

In order to quantify the relationship between vehicle performance, component selection, and energy consumption while accounting for a sizable number of drive cycles and already-produced EVs, the objective of this thesis is to model and simulate a three-wheeled, PMDC-motor powered electric vehicle. Another objective is to deploy high-performance vehicles powered by clean, renewable energy sources, utilising and generating as much as possible in a sufficient manner, and delivering a desired vehicle to the Ethiopian transportation sector. The proposed thesis's significance can be summed up as follows:

- Reducing greenhouse gas (GHG) emissions by replacing conventional vehicle with electric vehicle.
- Providing the high Performance and low power consume three wheeler electric vehicle.
- Increasing acceleration due to the electric motor's ability to move the car forward without waiting for the engine to start.
- Because EVs often have a lower centre of gravity and are therefore less likely to roll over, their safety features can be improved.
- Because it has fewer moving components than a typical car, maintenance costs are low.

1.7. Scope of the Study

Over time, the development of electric vehicles has grown to be a significant field. The following limitations apply to this thesis's scope because of time restrictions and the need to undertake a thorough analysis:

- In this thesis, only three-wheeled battery electric vehicles (BEVs) are taken into consideration. Fuel cell vehicles (FCV), plug-in hybrid electric vehicles (PHV), and hybrid electric vehicles (HEV) are not included because they mostly require additional research.

- The study is only focused on passenger’s three-wheeled electric vehicle; Fright three wheeled EV, Lorries, buses, etc. are not included.
- Modelling of the battery, controller, traction motor, and vehicle body has been done, as well as the design of the chassis. However, designing each component separately requires additional research, which was challenging because one component's parameters can affect another's power level.

1.8. Outline of the Thesis

Chapter 1: The introduction of electric vehicles, a statement of the problem, the study's objectives, significance, scope, and limitations are all covered in this chapter.

Chapter 2: Reviews of background-related literature and publications.

Chapter 3 discusses about the methods followed, thesis development techniques, Modelling of parts, and developing of the suggested system.

Chapter 4: The results of the suggested system are discussed in this chapter.

Chapter 5: The chapter ends with a conclusion and a recommendation.

CHAPTER TWO

LITERETURE REVIEW

2.1. Introduction

This chapter reviews and discusses the history and types of electric motors, the advantages of the PMDC motor over other electric motors and its widespread use in modern society, as well as the current regulation mechanism and other related uses of the PMDC motor. Sharad (Patel, 2016) after designing and analysing a three-wheeled campus mobility vehicle, it was determined that the design is secure against the appropriate range of load circumstances. After study, a number of parameters were recorded to assess the performance of the vehicle. The approach complies with the main criteria for campus mobility. (Ashish Kumar Singhal et al, 2015) Study was done on the SEPHV (Solar/Electric Powered Hybrid Vehicle), which uses energy that is stored in a battery and is charged by a solar panel.

The motor, which acts as the vehicle's engine replacement and pushes it in all directions, is powered by the charged batteries. By testing the SEPHV at an average speed of 40 km/h, its performance for a load of four passengers was found to be satisfactory. (Sharada Prasad N & K R Nataraj, 2014) The management of diverse energy sources, dependence on driving cycles, battery sizing, and battery management were listed as the main issues for HEV design. A prototype electric scooter was created using design and analysis. For further investigation, real-time traffic and speed were collected. (S.M.H.S. Omar et al, 2015) Presented a number of analyses to develop, improve, and manage the performance of an FC electric vehicle's powertrain for use in energy-efficient competitions.

The car was controlled, FC efficiency testing, vehicle dynamics modelling, track mapping analysis, DC motor characteristics, and driving strategy tactics were all tested previously. These made sure that the vehicle's powertrain system was sized optimally and that it was automatically controlled to run each component of the powertrain system at maximum efficiency. (Parag Kulkarni, 2015) Shows how there is a rising need for environmentally friendly transportation worldwide and how HEVs could play a part in finding a solution.

Some well-known automakers, including as Oldsmobile and Student Baker, really began as prosperous EV businesses before converting to combustion engine vehicles (Leitman.S, 2010). A lead battery that could be recharged provided the vehicle with the energy it needed to run.

In 1900, the United States produced about 4000 autos, 38% of which were electric, demonstrating that the electric car trend was at its height during this time. The 1920s had been the "golden age" of electric cars. Numerous technological advancements and advances, such as networks of charging stations, characterised this time period (Bhatta, P. et al, 2019). EVs, like other vehicles, were at that time primarily used in urban areas because electricity was readily available there. Compared to cars powered by combustion engines, EVs are quieter, safer, and easier to drive, which contributed to their early appeal.

The Columbia Runabout, which had a top speed of 15 mph and a range of 40 miles on a single charge, was one of the most popular EVs available at the time. When 34,000 automobiles were registered in 1912, the year of early EV production's peak, (Leitman, S., & Brant, B, 2009). But eventually, the cutting-edge battery technology was shelved as oil became more affordable and plentiful. As a result of conventional vehicles' competitive advantage, electric vehicles suffered. Up until the middle of the 1910s, EVs were a common sight, but the combination of cheap oil and the lack of electrification in rural regions ensured that combustion engine cars would eventually triumph over EVs.

A motorised assembly line and the addition of an electric motor to combustion engine automobiles, which eliminated the need for a risky and challenging crank to start the engine, are two other factors. Volume manufacture of combustion engine vehicles was also made possible in 1910. These circumstances led to the cessation of early EV production by the end of World War I (Bhatta, P. et al, 2019). However, with the invention of semiconductors and the introduction of different modifications to motors and controllers in the 1960s, interest in electric technology rose once more. (Ehsani, M. et al, 2005). The introduction of the first environmental rule during that time is also credited with the rise in popularity of electric vehicles.

According to information provided by Bhatta et al., 2019, and Anurag and Date, 2015, electric motors, such as DC Motor, Brushless DC (BLDC) Motor or Permanent magnet Brushless DC (PMBLDC) motor, Induction (AC) Motor, Permanent magnet Synchronous motor or PMSM, and Switched Reluctance motor (SRM), have been used in electric vehicles (EVs) up to this point. (Lulhe, A. M. & Date, T. N., 2015), (Porselvi, T., et al, 2017). An acceptable design mechanism for an electric vehicle and integration of various components that are employed in an EV structure was briefly explored based on the literature review that was summarised above.

It was discovered that the earlier simulation model (Abulifa, A. A., et al, 2017), (Lulhe, A. M. & Date, T. N., 2015) and (Kusum, 2018) Simulink block sets are used in MATLAB to produce diagrams that are comparable to their mathematical models.

To make a change, the simulated model in this paper was created using Simscape Block-sets and ansys, which uses a physical modelling approach and is analogous to connecting real components. This approach aids in understanding the physical connections between two components and provides a suitable representation of the physical system.

This paper depicts an accurate analogy of vehicle dimension derived from (Lulhe, A. M. & Date, T. N., 2015), (Porselvi, T., et al, 2017). Also, by considering the analysis (Berjoza, D. & Jurgena,, 2017), the weight and the capacity of the battery is considered. Based on (Xin. X., et al, 2020). To extend the analysis (Warake, K. et al, 2018), this paper includes an analysis of the three wheeler electric vehicle chassis using ANSYS software.

2.2. Three Wheeler Electric Vehicle

Previous related works on three wheeler Electric vehicles and other related electric vehicle implementations will be reviewed in this section. Although they are not particularly new to this planet, electric vehicles now have the reputation of being the form of transportation of the future thanks to technological advancement and growing concern over pollution. Electric energy serves as the primary source of power for driving in EVs. Electric motors in electric vehicles convert electrical energy into mechanical (rotational) energy. Through a suitable gearbox system, this rotational energy is coupled to a vehicle's wheels and provides drive.

Electric vehicles have two different power options: they can run solely on electricity or combine petrol engines and batteries. The three main parts of any electric vehicle are the battery, electric motor, and controller. Gustave Trouvé, a Frenchman, created the first electric vehicle in 1881. It was a tricycle with a lead-acid battery-powered 0.1 horsepower DC motor. (Ehsani, M. et al, 2005) . Due to their advantages over gasoline-powered vehicles, including as having no exhaust emissions, higher power efficiency, and lower maintenance costs, EVs can prove to be a very practical substitute for them. (Martins, F. et al, 2019).

2.3. Materials for Electric Vehicle Chassis Frame

The choice of materials for a vehicle is the first and most crucial factor in modelling of three wheeler power train. There are many materials that can be used in the automotive chassis, but the purpose of design is the main challenges here. The most important criteria that a material should meet are lightweight, safety, recyclability, economic effectiveness considerations (Singh, 2017).

Table 2. 1: Properties of Materials

Properties	Structural Steel	Aluminium Alloy	Magnesium Alloy
Mass (kg)	39.969	14.104	9.165
Density(kg/mm^3)	7.85*10^6	2.77*10^{-6}	1.8*10^{-6}
Poisson’s ratio	0.3	0.33	0.35
Young’s Modulus(MPa)	2*10^5	71000	45000
Bulk Modulus(MPa)	1.6667*10^5	69608	50000

The materials used in the cage must meet certain requirements of geometry and other limitations. The main criteria took into consideration when selecting the material for the roll cage safety, cost and durability (Satinder.S and Beant .S, 2014). After conducting the analysis in ANSYS it was found that for structural steel equivalent stress value is highest for circular cross-section and total deformation is lowest for square and rectangular cross-section. AISI 1020 is a low hardenability and low tensile carbon steel with Brinell hardness of 119 – 235 and tensile strength of 410 – 790 MPa. It has high machinability, high strength, high ductility and good weld ability. It is normally used in turned and polished or cold drawn condition. Due to its low carbon content, it is resistant to induction hardening or flame hardening.

2.4. Motors Used for Electric Vehicle

The majority of electric engines operate by the interaction of the motor's magnetic field and electric current in a wire winding to produce force in the form of torque applied to the motor's shaft. Electric motors can be powered by direct current (DC) sources, such as from batteries, engine vehicles or rectifiers, or by alternating current (AC) sources, such as a power supply. The heart of an electric vehicle is its motor, which supplies the crucial force for the vehicle's propulsion. Despite operating with a reversed control flow, an electric generator transforms mechanical energy into electrical energy. It is mechanically identical to an electric engine.

2.4.1. Different Types of Electric Motors Used in Electric Vehicles

Various electric motor types are compared based on a few factors that should be taken into account when choosing a particular motor type for an electric vehicle application. For some parameters, the comparison is tabulated. Additionally, many motors are mentioned at various locations on the attributes list.

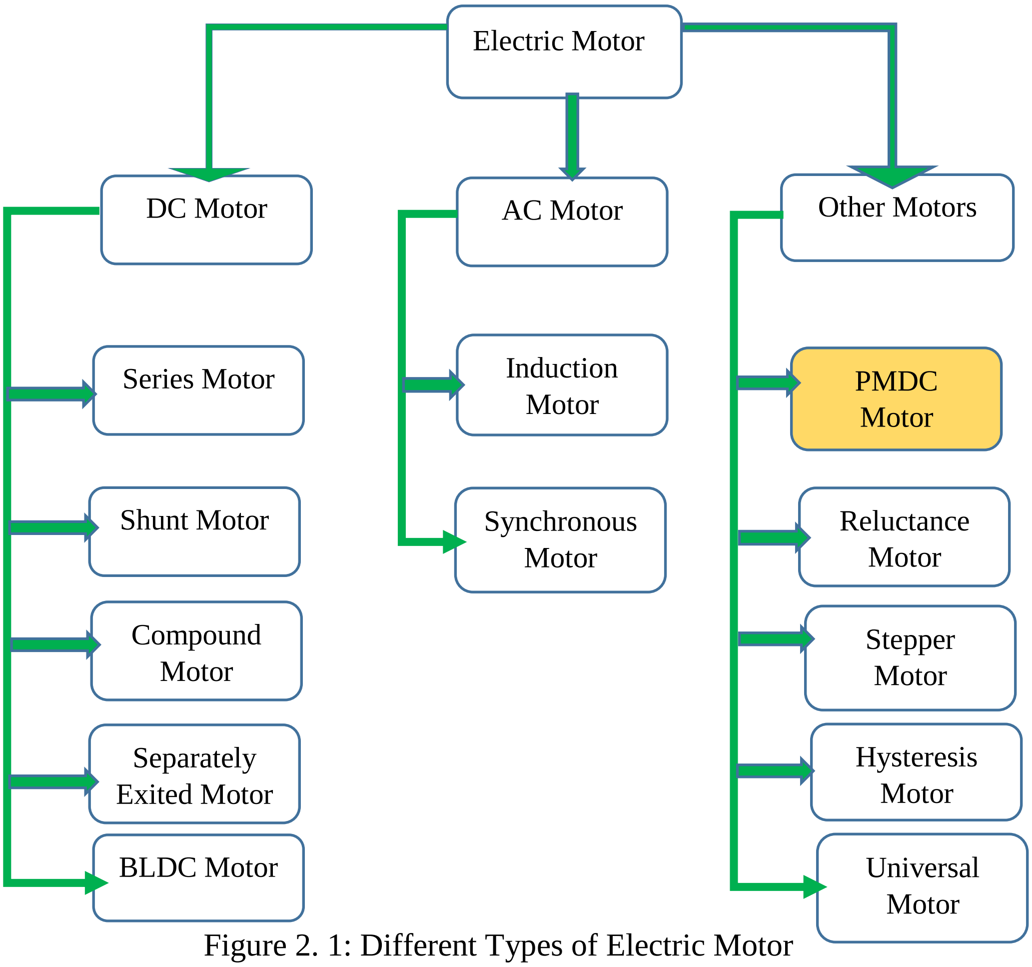

Figure 2. 1: Different Types of Electric Motor

2.4.2. Permanent Magnet DC Motor

We know that a DC motor has an armature which rotates within a magnetic field, and the main working principle of this motor depends on a current carrying conductor which is arranged in a magnetic field, and the mechanical force will be experienced with the conductor. DC motors are classified into different types which work on the same principle. Thus, the DC motor construction can be done by establishing a magnetic field with any kind of magnet like electromagnet otherwise a permanent magnet.

A permanent magnet is a component of a PMDC (Permanent Magnet DC motor), a type of DC motor that generates the magnetic field required for DC motor operation. It is possible to define a permanent magnet DC motor as a motor that has a permanent magnet pole. Instead of the field winding in this motor, the magnet can be employed to provide a flux that operates within the air gap. The rotor structure resembles that of a conventional DC motor. The rotor of a PMDC motor consists of an armature core, commutator, and armature winding.

A typical DC motor will often include two types of winding, such as armature and filed. While armature winding can be coiled on the rotor of the motor, the primary purpose of field winding is to produce the working magnetic flux within the air gap. Like in a typical DC motor, inactive carbon brushes are pressed against the commutator. The PMDC motor requires a DC supply of 6 volts, 12 volts, or 24 volts to operate, which is obtained from the voltage sources.

A cylindrical steel stator serves as a return channel for the magnetic flux and supports the permanent magnets of the PMDC motor. The rotor functions as an armature and contains brushes, winding slots, and commutator segments similar to those used in traditional dc machines. Alnico magnets, Ceramic (ferrite) magnets, and Rare-earth magnets are the three types of permanent magnets employed in this motor. Alnico magnets are used within motors which have the ratings in the range of 1KW – 150KW, Ferrite or Ceramic magnets are much cheap within fractional KW (kilowatt) motors and Rare-earth magnets are made with samarium cobalt as well as neodymium iron cobalt.

With the help of the permanent magnets in this motor, which are connected by a perpendicular field driven by the current flowing through the rotor windings, a mechanical torque can be produced. The position between the stator and rotor fields can be altered when the rotor spins in reaction to the generated torque, and the torque would be reversed in a 90 degree revolution. PMDC motors have a commutator attached to the rotor shaft to maintain the torque acting on the rotor.

In order to maintain a constant angle of 90 degrees between the two fields, the commutator activates the current supply towards the stator. Since each winding in the stator is regularly activated by the flow of current as the rotor turns, the frequency of the current exchange is proportional to the number of magnetic poles in the motor as well as the speed.

The following are some traits of PMDC motors. In terms of speed, torque, and armature current, the PMDC Motor characteristics are similar to the dc shunt motor characteristics. But in these kinds of motors, the speed-torque characteristics are more traditional and linear.

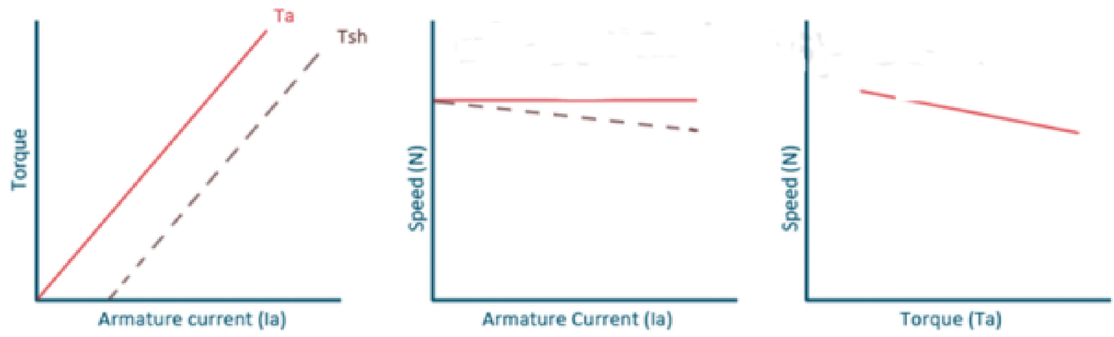

Figure 2. 2: PMDC motor characteristics (J.Chapman, 2007)

In a DC brushed motor, the armature and the external supply circuit are connected by the brushes and commutations. Brushes are typically rectangular in shape and can be constructed of carbon, copper, carbon graphite, or metal graphite. (J.B.Gupta, 2015). One of the primary problems of DC brushed motors is the wear on the commutations caused by the constant cutting of the brushes. The maximum motor speed is also restricted by friction between brushes and commutations. DC brushed motors are appropriate for traction systems because they can provide a lot of torque at low speeds. (X. D. Xue and N.C Cheung, 2008).

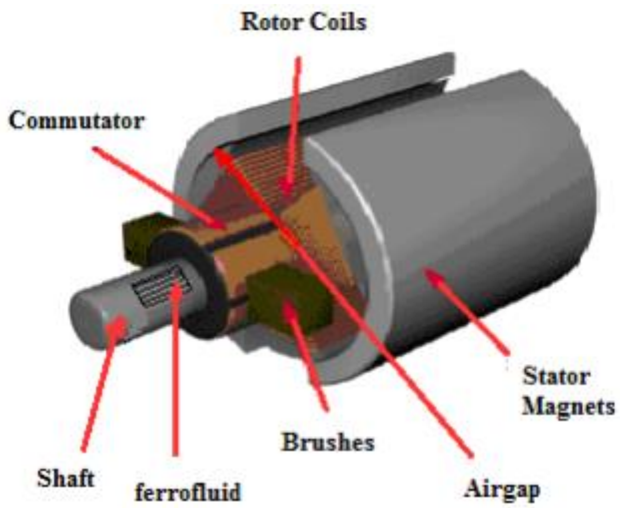

Figure 2. 3: Permanent Magnet DC Motor (J.Chapman, 2007)

2.4.3. Asynchronous Induction Motor

Due to its great efficiency, excellent speed regulation, and lack of commutations, three phase induction motors are frequently utilised in electric cars. Stator winding is coupled to a three-phase AC source, creating a rotating magnetic field. Induced current flows through the stationary rotor conductors as a result of the interaction between the rotating magnetic field and the conductors. An induced current creates a magnetic field of its own. Unidirectional torque results from the interaction of the magnetic field, which is rotating, and the field caused by induced currents (X. D. Xue and N.C Cheung, 2008) . These motors are also known as asynchronous motors since the rotor's speed is different from (less than) the speed of the rotating field (synchronous speed).

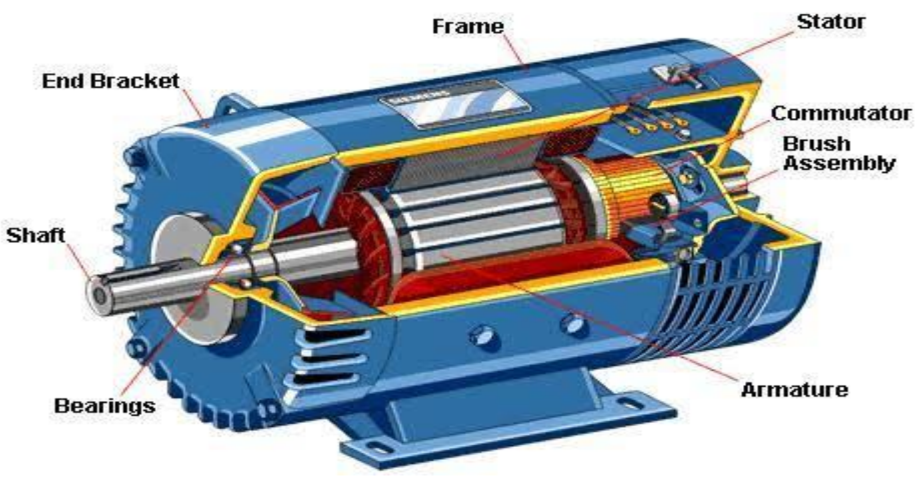

Figure 2. 4: Induction Motor (J.Chapman, 2007)

2.4.4. Switched Reluctance Motor (SRM)

By using a variable reluctance approach, switched reluctance motors generate torque. Variable reluctance is created in the space between the stator and the rotor when the stator coils are powered up. Torque is produced when the rotor moves to the point with the least resistance. High starting torque, a wide speed range, and improved inherent fault-tolerance make switched reluctance motors appropriate for use in electric vehicle applications (Cheng He, et al, 2016). Power-to-weight ratio, torque-speed characteristics, efficiency, cost of the controller, and motor cost are some factors that must be considered while comparing the aforementioned motors to determine which one is best suited for the needed electric vehicle application (RuiEstevesAraújo, et al, 2005).

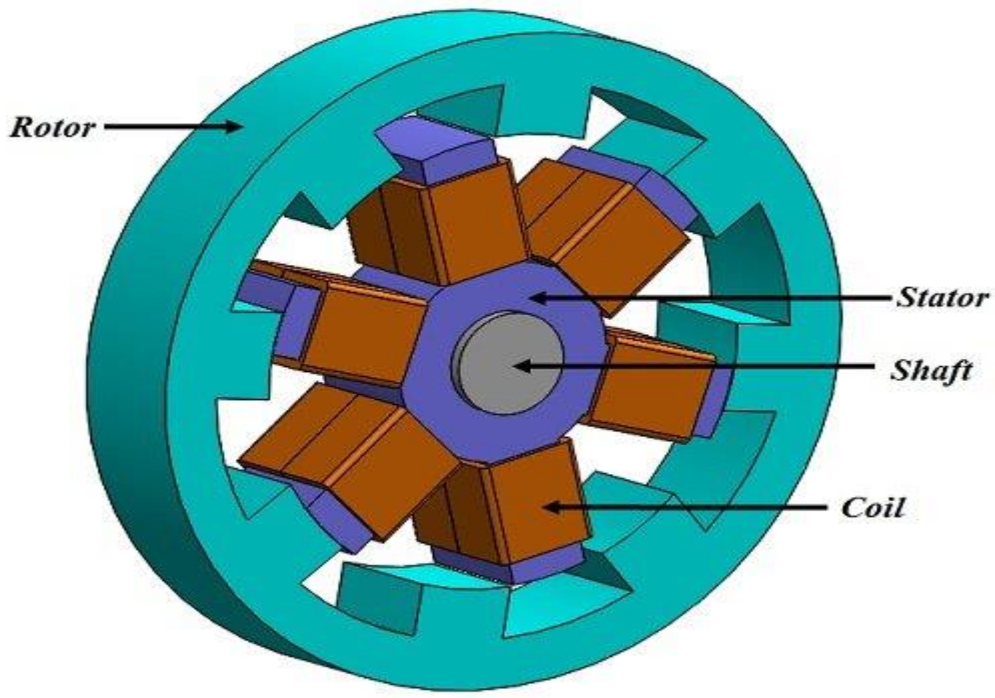

Figure 2. 5: Switched Reluctance Motor (J.Chapman, 2007)

2.4.5. Brushless DC Motor (BLDC)

The mechanical commutation present in brushed DC motors is replaced with an analogous electronic commutation (inverter circuit and rotor-position sensor element) circuit in brushless DC motors, leading to benefits such as less maintenance and improved efficiency (X. D. Xue and N.C Cheung, 2008) (M.V.Ramesh, et al, 2000) . As a revolving self-synchronous machine with a permanent magnet rotor and known rotor shaft positions for electronic commutation, a brushless DC motor is described. (D. van Niekerk and D.V. Nicolae, 2015). Compared to other motors, brushless DC motor offers more torque at its peak current and voltage values (M.V.Ramesh, et al, 2000). These motors are used in ventilation systems, pumps, and compressors because they operate more effectively at greater speeds.

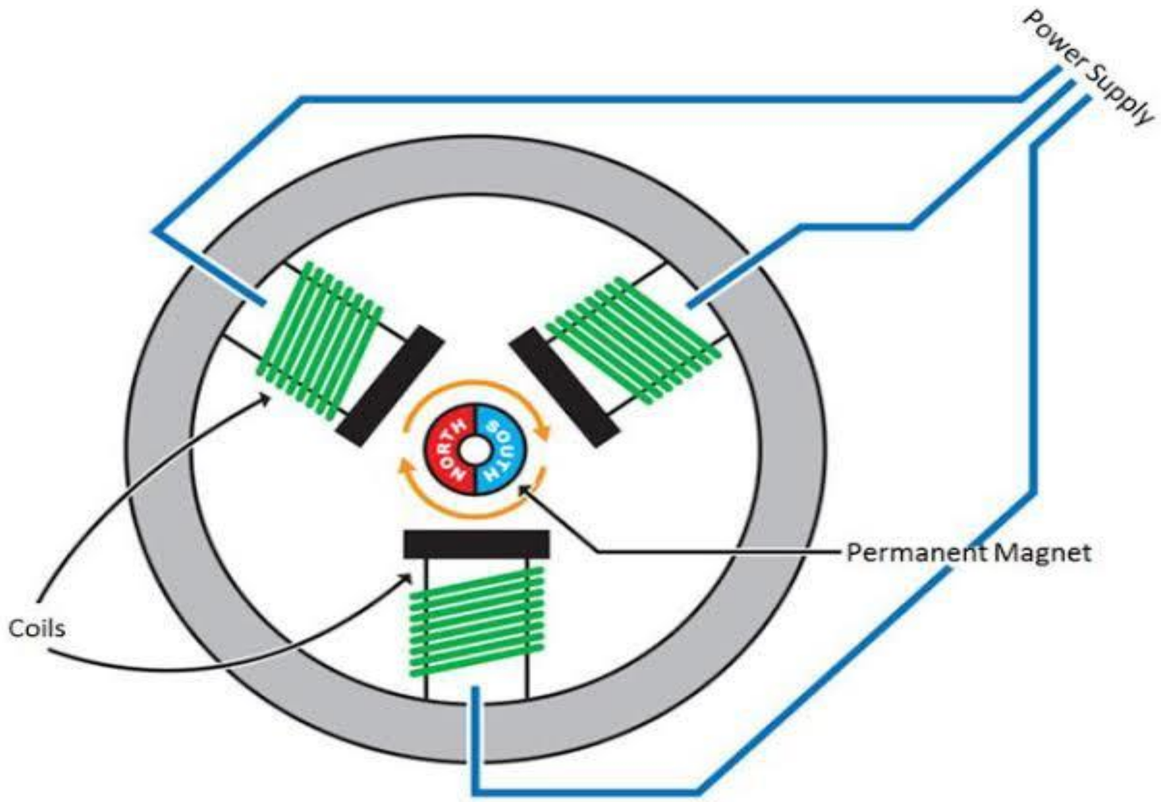

Figure 2. 6: PMBLDC Motor (J.Chapman, 2007)

2.4.6. Permanent Magnet Synchronous Motor (PMSM)

Additionally, this motor resembles a BLDC motor because it features permanent magnets on the rotor. These motors share traction features with BLDC motors, such as high power density and good efficiency. The distinction is that the back EMF of PMSM is sinusoidal while the back EMF of BLDC is trapezoidal. Enduring magnet higher power ratings are possible with synchronous motors. For high performance applications like vehicles and buses, PMSM is the optimum choice. Despite being more expensive, PMSM is giving induction motors a tough fight because of its higher efficiency. In addition, PMSM costs more than BLDC motors. PMSM motors are used by the majority of automakers in their hybrid and electric vehicles. For instance, PMSM motors are used in vehicles like the Toyota Prius, Chevrolet Bolt EV, Ford Focus Electric, zero bikes S/SR, Nissan Leaf, Honda Accord, BMW i3, etc.

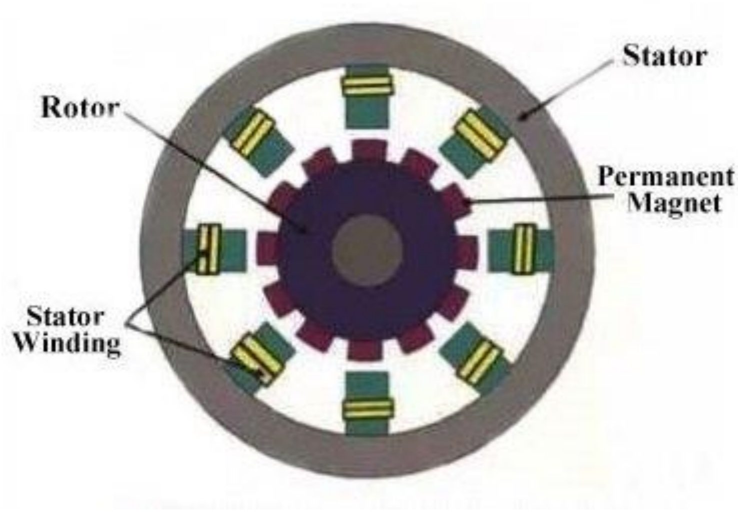

Figure 2. 7: Permanent Magnet Synchronous Motor (J.Chapman, 2007)

2.5. PMDC Motor and Other Motors in Comparison

The only issue with electric-powered vehicles is that they require significantly more battery power for large-capacity drives. Therefore, the lesser capacity drives' primary use is in this scenario. The needed motor must use the electrical input and be driven by a suitable controller because the input power is electrical. Choosing the proper motor is crucial since the reliability of the motor is also crucial.

Induction motors are better suited for applications requiring a single speed, but if the speed must be maintained as the load varies, PMDC motors are a viable choice due to their flat speed-torque curve. Due to the additional controller that variable speed induction motors require, which raises the cost of the system, PMDC motors become a better fit for certain uses. Due to ongoing maintenance, brushed DC motors will also be a more expensive alternative.

However, BLDC motors need optical encoders for these applications, and sophisticated controllers are needed to track torque, speed, and position. BLDC motors are a better fit because brushed DC motors are recognised for producing more EMI noise; nevertheless, the controlling needs for BLDC motors also produce EMI and audible noise. On the basis of comparative analyses shown in Tables 2.1, 2.2, and 2.3, the PMDC was chosen as a suitable motor.

Table 2. 2: Comparison of Different Types of Electric Motor

Futures	**BLDC Motor**	**PMDC Motor**	**Induction Motor**
Speed-Torque Characteristics	Flat in nature as the result it can operate at all speeds with rated load	Moderately flat, at higher speed brush friction increases reduction of useful torque	Non-linear, it enables lower torque at lower speeds
Efficiency	High	Moderate	Less
Rotor Inertia	Lower and hence better dynamic characteristics	Higher and hence limited dynamic response time	Higher and hence poor dynamic characteristics
Electric Noise	Less	High because of brushes	Less
Speed range	Higher no loses in brushes	Moderate loses in brushes	Lower determined by the AC line frequency increases in load further reduces speed
Control requirements	A controller is always required to control the commutation sequence	No controller is required for a fixed speed, controller required for variable speed	No controller is required for a fixed speed, controller required for variable speed
Commutation Method	Using solid state switches	Mechanical contacts between brushes and commutation	The special starting circuit is required
Maintenance	Less Maintenance	Periodic maintenance because of brushes	Less maintenance
Cost	Expensive	Cheaper	Cheaper

Table 2. 3: SRM and PMDCM comparison

Parameter	PMDCM	SRM
Power Density	Higher	Lower
Air gap	Up to 1mm or more	Small, fraction of mm
Efficiency	Over 90%	Low
Performance at low speed	Good	Torque is high, but low efficiency
Torque ripple	About 10%	Over 20%
Power electronics converter	Necessary	Necessary
Cost	Still expensive motor	Cost effective motor

Table 2. 4: Comparison between PMBLDCM and PMSM

Parameter	PMBLDCM	PMSM
Machine Type	Synchronous Machine	Synchronous Machine
Back EMF	Trapezoidal	Sinusoidal
Rotor Position sensor	Stator flux position commutation each 60^0	Continuous stator flux position variation
Phase Winding energized	Only two phases ON at the same time	Possible to have three phases ON at the same time
Torque ripple	High	Moderate
Switching Losses	Less Switching losses	High switching losses at the same switching frequency
Control algorithms	Control algorithms are relatively simple	Control algorithms are mathematically intensive

In comparison to an induction motor, SR motor, and synchronous motor, the aforementioned analysis demonstrated that a PMDC motor is the best option for three-wheeled electric vehicles. PMSM motors are more effective, quieter, and have less torque ripple. However, because it is more difficult to manage, has higher switching losses at the same switching frequency, and is more expensive than PMDC motor, it is not suggested to use PMSM for electric vehicles.

2.6. Electric Vehicle Batteries

A battery electric vehicle (BEV)'s electric motors are powered by an electric-vehicle battery (EVB), in addition to traction batteries designed specifically for industrial (or leisure) vehicles. Smaller, lighter batteries enable electric vehicles to be lighter and perform better by reducing the vehicle's overall weight while maintaining a high power-to-weight ratio, specific energy, and energy density. Most modern battery technologies have substantially lower specific energies than liquid fuels, which frequently affects the cars' maximum all-electric range. However, because the cathode is given by the surrounding oxygen in the air, metal-air batteries have high specific energy.

2.6.1. Types of Electric Vehicle Battery

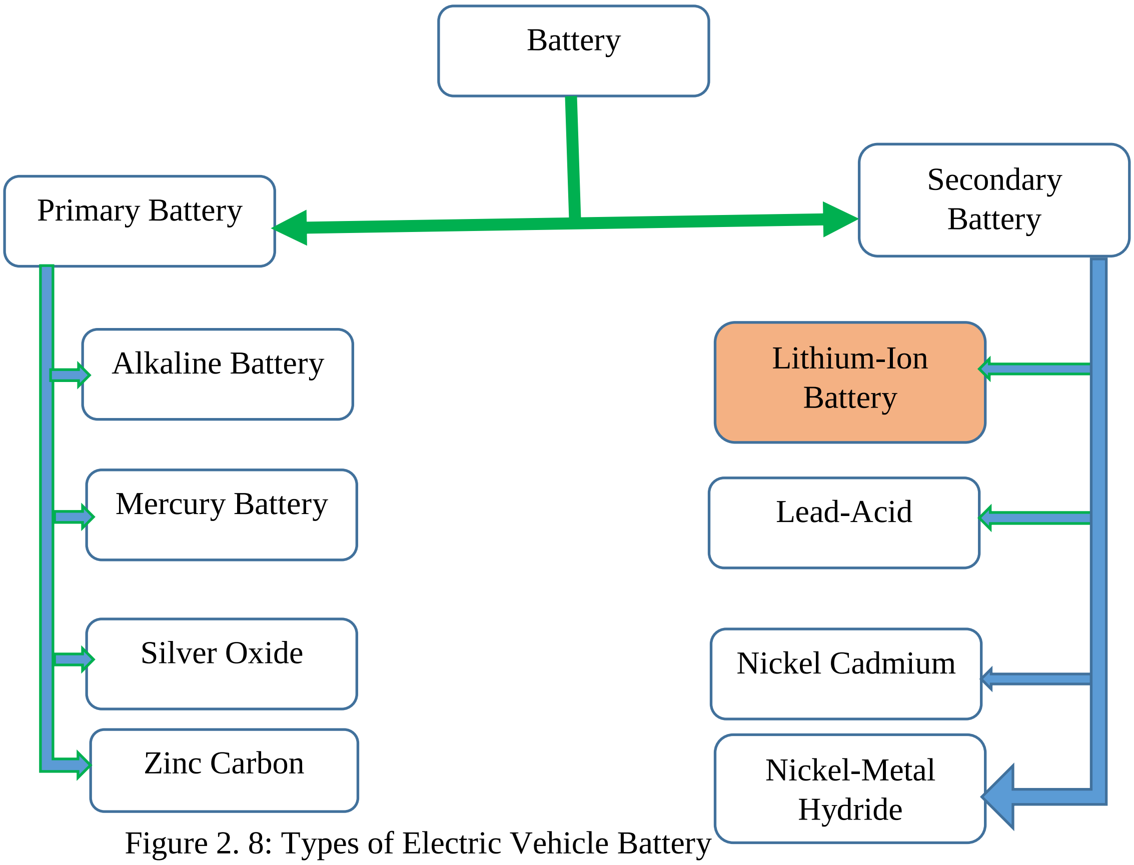

Figure 2. 8: Types of Electric Vehicle Battery

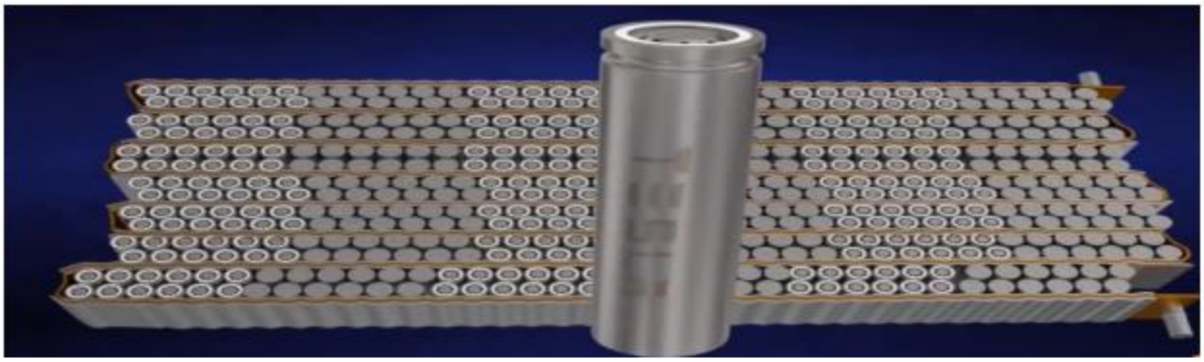

Figure 2. 9: The battery Pack (Tendillo, 2015)

2.6.2. Comparison of Electric Vehicle Batteries

For electric vehicles, lithium-ion batteries have better performance metrics than other types of batteries. Compared to the majority of other usable batteries, it has a better energy density, a longer lifespan, and a higher power density. Safety, durability, heat breakdown, and cost are complicating elements. To function safely and effectively, Li-ion batteries must be used within safe temperature and voltage ranges (Hua J. and Ouyang M., 2012). In terms of battery technology, there are many different varieties, and each has advantages and disadvantages. However, in the case of green energy, it is up to the engineer to choose the battery that best fits the desired design, taking into account a variety of variables like the reactant concentration, temperature, and range of reactions that may have an impact on the charging and discharging phase of the battery bank.

Compared to all other non-toxic rechargeable batteries, lithium batteries provide excellent energy densities. The primary drawback of lithium batteries is how long they take to charge. However, research is looking at quick battery charging. The goal of their efforts is to develop a crystal structure that would charge conventional lithium batteries one hundred times more quickly (Negash, 2017).

Both conventional large-scale power utility applications, including backup systems, and renewable energy sources, such extensive photovoltaic regions and wind farms, use zebra cells. Because they are less expensive than li-ion batteries, zebra cells are typically more competitive. It takes 6 hours for zebra cells to reach their maximum load in regular mode. They may be fully charged in about one hour using the quick charge option. (Kumar, 2017).

Lithium-ion Batteries Concentrated solar power may now be stored in molten salt, enabling it to be generated on demand and to supplement intermittent sources of electricity like wind and solar power. The molten salt is a great electrolyte that is perfect for battery operation since it is non-volatile, non-flammable, and has a high ion and energy density. This battery's sole significant flaw is its need to operate at high temperatures.

Table 2. 5: Comparison of Different Types of Electric Vehicle Batteries

No	Types of Battery	Advantages	Disadvantages
1	Lithium-Ion Battery (Li-Ion)	High energy density, High power rate , Cycle Life Longer run time , High efficiency, No loss of amp hours	Expensive Technology not properly developed
2	Lead-Acid (Li-S)	High power density, Medium efficiency, Loss of 55 amp Hours, Reliable and cheap	Low energy density, High maintenance Very large and old type bulky
3	Nickel-Cadmium (Ni-cd)	Good life cycle Available in different size	Low output voltage Expensive and Toxic
4	Nickel-Metal Hydride (Ni-MH)	High capacity Energy density same size	More complex, Charging algorithm needed, High self-discharging, Low power rate

2.7. Related Work on PMDC Motor Speed Control

In order to employ DC motors, which have emerged as the most crucial machine in control systems, it is advantageous to convert alternating current into direct current in the majority of electrical appliances found in homes and in specific applications such as in trains, electric cars, and process control (J. Santana, et al, 2002). The rationale is that DC motors have better speed and torque characteristics than AC motors (Benjamin.C, 2011). Due to their affordable price and simplicity of operation, DC motors are particularly preferred in high power and precise servo applications (J. Ruderman, et al, 2008).

A PMDC motor does not experience any interaction between the permanent magnet's field and the armature demagnetizing cross field, in contrast to a shunt wound DC motor (R. Bullock, 2001). They can produce significant transient starting and acceleration torques as a result of the lack of armature interaction, generally 10 to 12 times the entire rated torque (R. Bullock, 2001). Because of this, PMDC motors are appropriate for applications that need high starting torques. However, they are not meant to operate continuously at such high torque levels since this could lead to overheating and irreversible demagnetization of the field magnets (R. Bullock, 2001).

Its speed must be managed in order to control the current and subsequent torque because of this the speed of a DC motor was managed using a cascade structure with a Generic Model Control (GMC) in the inner loop and a PID in the outer loop (Abd-Elhamid, 1680-1688). The output of the current response chattered when a load of 12Nm torque was applied, and there was a significant overshoot. Shaft position chattering endangers the motor's lifespan and, by extension, the system.

Similar studies examined the capabilities of an intelligent self-tuning PI cascade controller and a standard PI cascade controller (M. N. Kamarudin and S. M. Rozali, 2008) .The auto-tuning PI controller provided a better settling time when a load is applied, according to the results. We employed a self-tuning PI cascade in (M. N. Kamarudin and S. M. Rozali, 2008) because it is challenging to perfectly tune the PI parameters without a thorough understanding of the behaviour of the system to be controlled and, consequently, without a good mathematical model of the system.

There are numerous DC motor models that can faithfully reproduce machine behaviour, however for the mathematical model to provide the desired behaviour, the model parameters must be properly set (A. A. Bature, et al, 2001), (Yildiz, 2012). The typical single PI controller, among the other evaluated controllers, was carefully adjusted to achieve satisfactory results after establishing a good mathematical model because of their cost effectiveness in comparison to its auto-tuned competitors.

2.7.1. H-Bridge with PWM control of DC motor

Many electrical or control systems frequently use brushed DC motors. For example, brushed DC motors are used in battery-operated hand drills, robotic applications, ink jet printers, electric trains, and wheelchairs for the crippled. Because of their affordability and simplicity, brushed DC motors are frequently chosen (Hughes, 2006). At the DC motor applications, DC motors must be controlled. The drive circuit must be designed in order to manage the motor's intended speeds and whether it should move forward or backward for varied lengths of time.

The operation of a brushed DC motor does not require an external driver, making it very simple to manage. Because the voltage-speed characteristic of brushed DC motors is largely linear, speed control of these motors is similarly simple (Hughes, 2006) . Typically, DC motors attempt to be controlled by a transistor-connected variable resistor or potentiometer. The primary issue with the control mechanism that uses transistors is that these transistors heat up. The efficiency of this motor driving system is reduced as a result of the transistor system's power being wasted outside due to warmth. To overcome this drawback it is possible to operate a DC motor using pulse width modulation (PWM).

By using brief pulses, the PWM DC motor control method modifies the motor speed. The "Duty Cycle" refers to the fill rate of these PWM pulses. The speed of the motor can be altered in accordance with Duty Cycle. The motor spins more quickly if the duty cycle is high; conversely, if it is low, the motor spins more slowly. (Gupta, 2010). On the basis of an operational amplifier type LM324, Jamal A. Mohammed created and executed a motor bi-directional DC control circuit using pulse width modulation (PWM) (Mohammed, 2013). In their investigation, Nicolai and Castagnet demonstrated how a microcontroller may be utilised for speed control. The PWM signal from a microcontroller unit drives a chopper as part of the drive for a rectified voltage (Castagnel, 1993).

Bi-directional brushed DC (BDC) motor control using the Enhanced, Capture, Compare, and PWM (ECCP) on the PIC16F684 was covered by M. Rylee.R. Karthick created a circuit that enables parallel port control of a DC motor's speed (Karthick, 2004). The motor speed was managed by a piece of software running on the PC. M. George proposed a separately excited DC motor speed controller with variable armature voltage (George, 2008).

PWM signals are typically used to control the speed and rotational direction of DC motors. The applied voltage to DC motor windings can be adjusted using PWM signals. This variation is interpreted as a motor speed. The speed increases as the voltage rises. Pulse width modulation

(PWM) is employed in many applications where simple voltage regulation would result in significant power loss in the control circuit. In order to reduce switching transition time and related switching losses, the semiconductor power devices are turned on or off as quickly as is realistically possible thanks to the rapid rising and falling edges.

The switch between supply and load is quickly turned ON and OFF to adjust the average value of voltage provided to the load. The power provided to the load increases with the length of time the switch is ON compared to the length of time it is OFF. A low duty cycle equates to low power because the power is OFF for the most of the time. The word duty cycle reflects the proportion of ON time to the regular interval or period of time. Duty cycle is measured as a percentage of total ON time. The PWM signal logic is illustrated in Figure (2.10). The "duty cycle" is a measure of this "on" time that is expressed as a percentage and is determined as follows:

Duty Cycle (%) = on time / Period x100 (1)

With a duty cycle of 25%, 50%, and 75%, the average perceived voltage of these PWM signals is shown in Figure 2.10 to correspond to various voltage levels. The reciprocal of the period is used to compute the frequency of the PWM drive signal (Rashid, 2004):

PWM Frequency = 1 / Period (2)

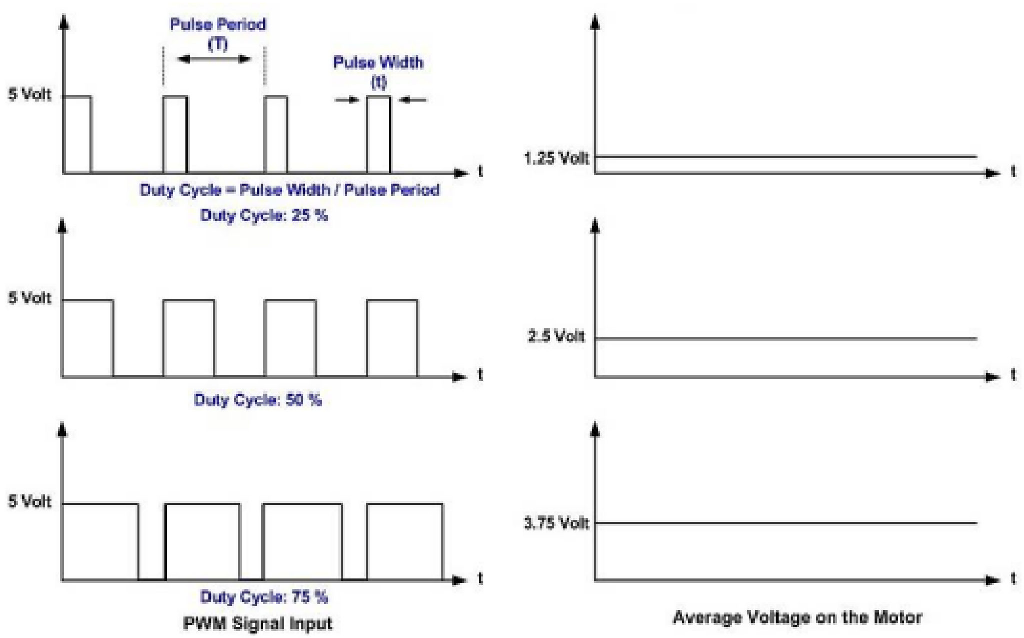

Figure 2. 10 : PWM Timing diagram (Wu,Licheng, et al, 2011)

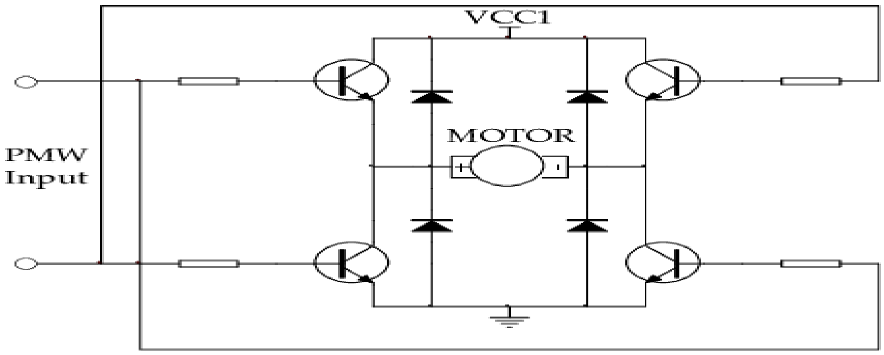

Figure 2. 11: H-Bridge circuit for DC motor control (Wu,Licheng, et al, 2011)

2.7.2. Bidirectional DC-DC Converter

Figure 2.12 displays a bidirectional buck-boost converter. The primary distinction between a unidirectional DC/DC converter and one that switches the current's state using MOSFETs or IGBTs as opposed to all diodes (Bhajana, V. V., and Pavel Drabek, 2015). The bi-directional DC-DC converter can operate as a Buck converter by stepping down from a higher voltage to a lower voltage or as a Boost converter by stepping up from a lower voltage to a higher voltage, depending on the magnitude of the voltage and current as well as the placement of the energy storage items. Although diodes do not permit current to flow in both directions, MOSFETs make it simple to control the time of each position (Gupta Gaurav and Prerna Gaur, 2015).

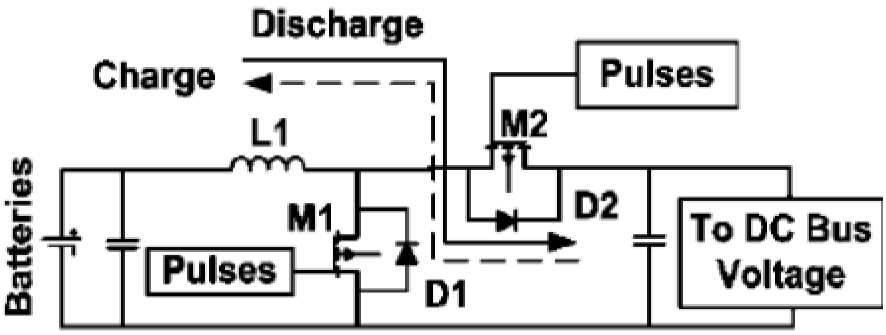

Figure 2. 12: Bidirectional DC-DC Convertor (Gupta Gaurav and Prerna Gaur, 2015)

In contrast to other techniques, this one converts kinetic energy into rectified electric energy that is then stored in a rechargeable battery for use in automotive applications, where most DC/DC converters are required to switch power between two voltage sources (Atul Kumar and Dr. Prerna Gaur, 2014). Current must be able to flow across the circuit in both directions in order to transfer this power. The use of a bidirectional converter enables avoiding a complex system of twin circuits to achieve the charge and discharge of the battery. There are numerous techniques for this type of converter because the use of a battery implies the capacity of charging and discharging.

2.8. Related Works on Electric Vehicle Battery

A thorough examination of various electrical energy storage technologies appropriate for use in vehicles was conducted in (M. Hannan, et al, 2017) and (G. Ren, et al, 2015). Various battery technologies, such as Li-ion batteries, lead acid batteries, Ni-MH batteries, and ultracapacitors, are available for electric cars (S. Manzetti and F. Mariasiu, 2015) . When compared to lead-acid batteries, lithium-ion batteries produce the lowest operating costs and GHG emissions.

2.9. Summary of Reviews

Table 2. 6: Summary of Reviews

Author	Objectives	Key Findings
(Jayakaran, 2017)	Design and Analysis of cost and weight reduced suspension system for cargo three wheeler electric vehicle	The result shows that the deflection of the spring is improved and stiffness is reduced and the design is safe.
(Xin. X., et al, 2020)	SOC determination	The authors compared the extended Kalman filter algorithm with Kalman filter and coulomb counting.
(Bhatta, P. et al, 2019)	Analysis of efficiency, power density, and size of EV	For all the characteristics PMBLDC motor shows the best results.
(Lulhe, A. M. & Date, T. N., 2015)	Speed controller and PWM inverter designing	The paper uses the MATLAB Simulink software to create and simulate an electric vehicle employing an induction motor.
(Abulifa, A. A., et al, 2017)	SOC determination	The simulated model for EV created with MATLAB Simulink software is included in the study.
(Kusum, 2018)	Powertrain Components	The suggested approach comprises EV simulation and design using the MATLAB programme.
(Porselvi, T., et al, 2017)	Motor rating analysis	The vehicle dynamics are used to determine the power rating of an EV, and ANSYS Maxwell Software is used to determine the motor speed.
(Patel, 2016)	Design and Analysis of three wheeler campus mobility vehicle	The Finding came to the conclusion that the design is safe against the corresponding diverse load circumstances after all the analysis and design calculations.

2.10. Research Gap

The following are the gaps in the literature:

- Most of the studies were done on freight three wheeler electric vehicles for which the result of analysis is somewhat different from passenger three wheel electric vehicles.
- Many researches done focused on one parameters such as determining state of charge, analysing performance of motor, and analysing battery for electric vehicle.
- Three wheeler electric vehicle studies in most of the literature review are done using Induction motor as electric motor drive which are less efficient, nonlinear speed-torque characteristic than that of DC motor.

CHAPTER THREE

MATERIALS AND METHODOLOGY

3.1. Introduction

The characteristics and attributes of the materials and software utilised were detailed, data analysis was included, and along with a description of the methods the thesis was finalized. Modelling of every components to create the entire system were also covered in this chapter. Finally, the system was simulated using software such as MATLAB Simulink, SolidWorks and ANSYS.

3.2. Methods

The supply (Battery), the PMDC motor and it's Controller, the DC-DC voltage converter, and the three-wheeler vehicle body make up the thesis work. The accompanying figure 3.1 provides a general illustration of this suggested system.

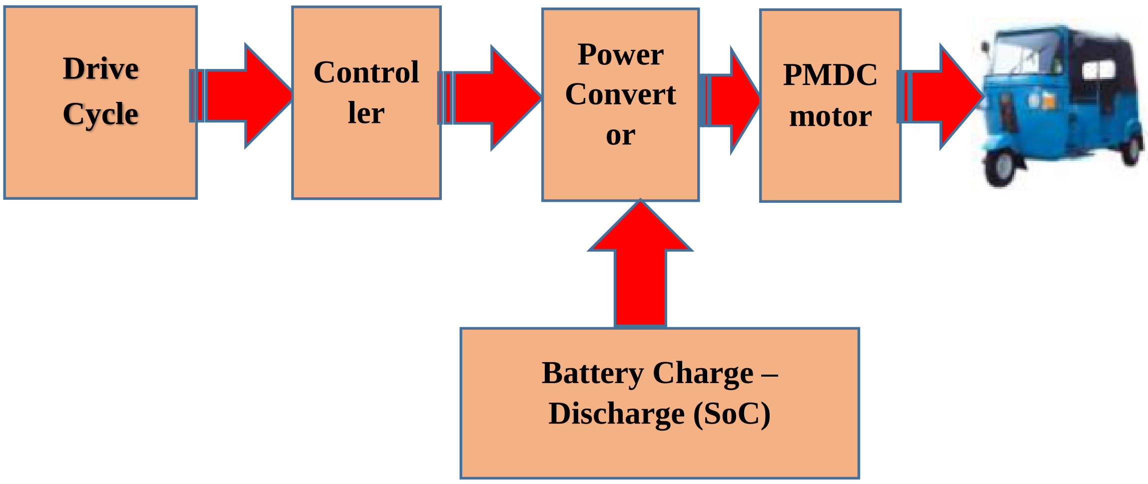

Figure 3. 1: The General Block Diagram of the Thesis

The overall and focused goals of this thesis are achieved using the following methodology. The closely connected works are examined first. The relevant information for this study is then obtained from an electric vehicle manufacturing company via their website. The acquired data is next evaluated in order to comprehend and develop the system models. The mechanism for developing a three-wheeled electric vehicle powered by a PMDC motor is modelled in its entirety. The system was simulated using the software Matlab/Simulink and ansys. The method used for the entire thesis study can be summed up as the flow chart below.

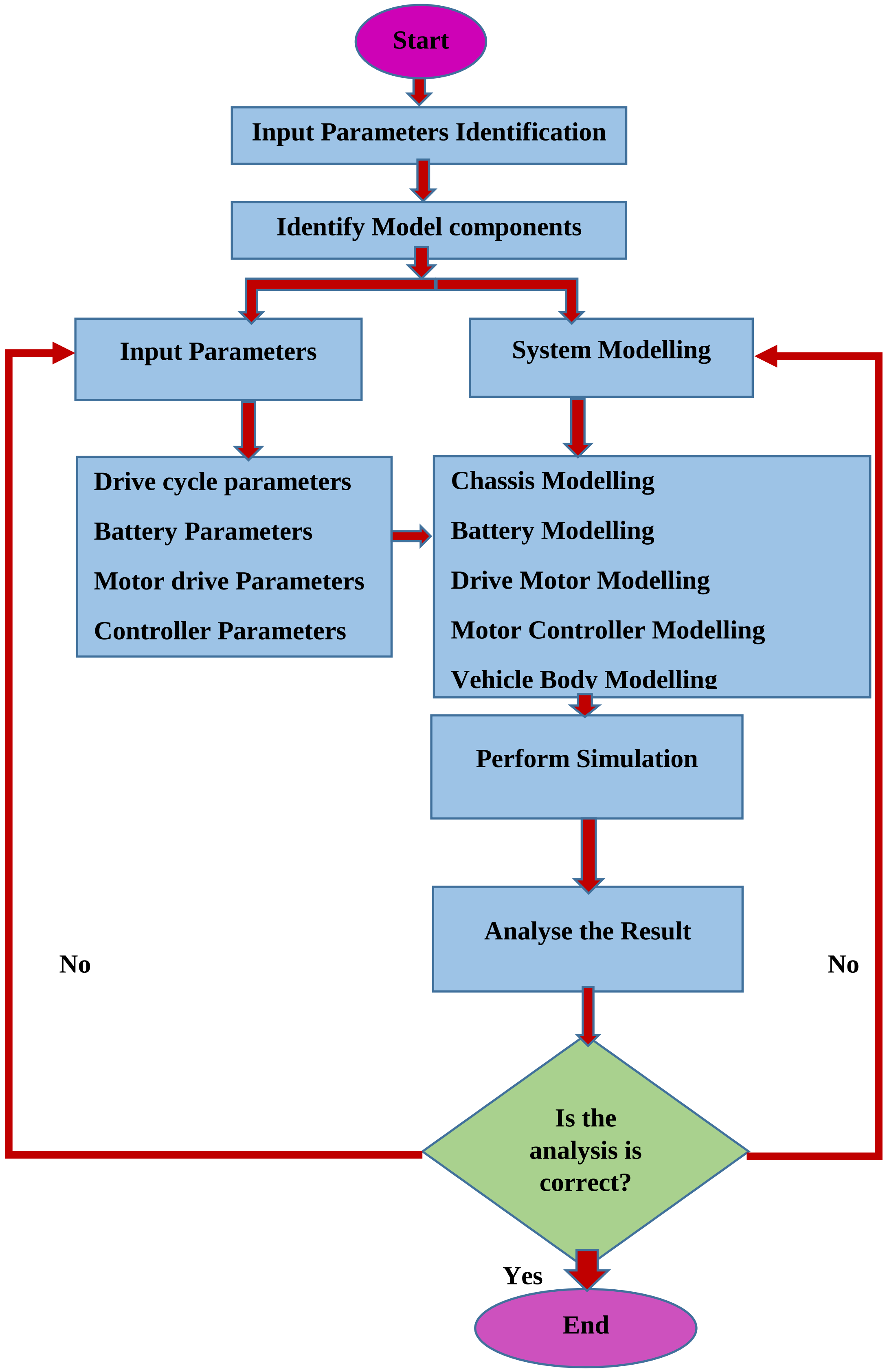

Figure 3. 2: Thesis Flow Chart

The PMDC motor is similar to an ordinary DC shunt motor except that its field is created by permanent magnets instead of salient-pole wound-field structure.

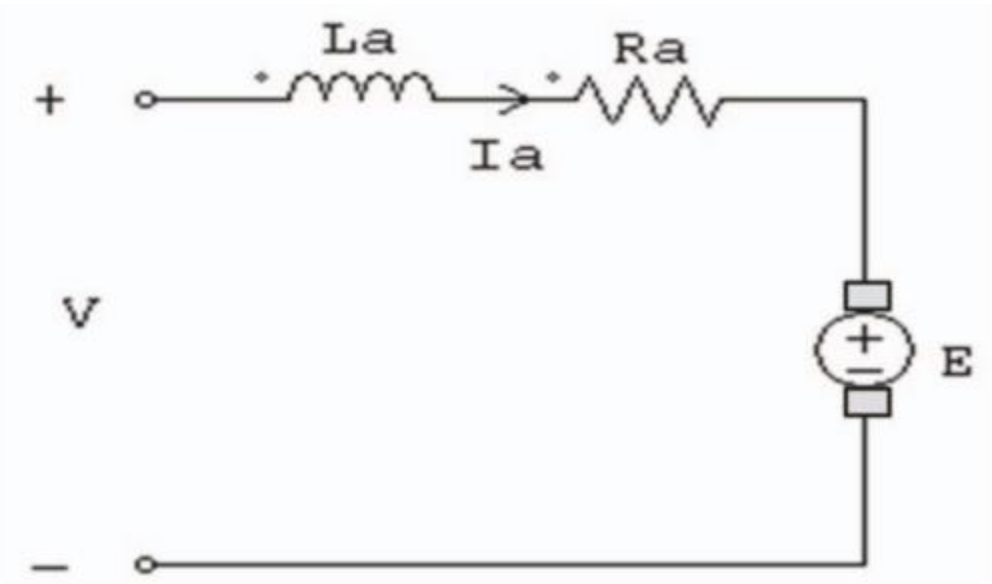

Figure 3. 3: Circuit diagram of PMDC motor *(S.M.Baque Billah and K.K.Islam, 2016)*

The common basic two equations of PMDC motor are:

$$E = K \times \varphi \times \omega \quad (1)$$

$$T = K \times \varphi \times I_A \quad (2)$$

I_A = armature current (amps)

φ = field flux per pole (weber)

E = Back E.M.F voltage (volts)

ω = angular speed of dc motor (rad/sec)

K = constant that relates to construction of dc motor

T = induced torque (N.m)

Ra = armature resistance (ohm)

La = armature inductance (H)

Armature current is given by:

$$I_A = V\text{-}E / R_a \quad (3)$$

In equation (3)

V = motor armature voltage

Now rotational speed of PMDC is proportional to motor armature voltage and speed is controlled by applying variable armature voltage. If V1 and V2 are two different armature voltages. Those voltages will generate two different speeds N1 and N2 rpm and two back E.M.F voltages E1 and E2 simultaneously. If V1 > V2 then also N1 > N2 and from equation (1) E1 > E2. Now if a motor feed with V1 voltage then its speed will be N1 rpm. During this running condition if we change the motor armature voltage V1 to V2 using different battery cell then E1 > E2 and based on equation (3) $I_A < 0$ that means motor will works as a generator (Regenerative mode) and charge the battery cell (which voltage is V2) until motor achieve the speed N2 and back E.M.F E2 . Now based on equation (2) and (3) T < 0 which indicates motor will experience a braking torque T during this regenerative mode and comparative to difference of rotational speed. This extra rotational or kinetic energy is converted into electrical energy and return back to the battery system. Based on this different armature voltage technique an effective regenerative braking system of PMDC motor can be developed.

3.3. Materials Used

In this topic, the study was going through each of the crucial components individually. Additionally, go over each component's physical attributes and features that are necessary for this thesis to function. As the system is built from a variety of elements, each entity's requirements are gathered. Additionally, each component has a unique operating principle and operation that it uses in specific situations to carry out defined functions. Various materials those are found in Matlab-Simulink Library and ANSYS library which are used to execute the thesis work for designing, modelling and analysis are explained briefly as below. Since chassis is the backbone of the electric vehicle the material used for modelling the chassis frame is the structural steel.

The geometry must first be cleaned up in order to establish connectivity before performing the normal finite element analysis of the chassis. This section adheres to the guidelines. The rectangle of the channels used in the chassis frame are 80 x 40 x 3 mm and 60 x 40 x 3 mm, respectively. Electric vehicle chassis geometry is modelled with SolidWorks software.

Material for the necessary chassis cross rails and side rails are 80 x 40 x 3 and 60 x 40 x3 mm rectangular box channels. To select the best potential material, study was done. The material

AISI 1020 is selected for the chassis frame as specified in reference literature the availability, mechanical properties and cost. Cost, availability, performance, and material weight were taken into consideration when choosing the material. The benefits of adopting rectangular box channel, which has good bending and torsion properties. Table 3.1 below depicts the mechanical characteristics of a rectangular steel channel.

Table 3. 1: Material Properties and Composition of Structural Steel

S.No	Structural steel parameters	Value	Units
1	Density	7850	Kg/m^3
2	Poisson's ratio	0.3	-
3	Carbon%	0.18 – 0.23	-
4	Young's modulus	200	GPa
5	Yield stress	250	MPa
6	Ultimate Tensile Strength	460	MPa
7	Reference Temperature	22	C^o

3.4. Dynamics of Three Wheeler Electric Vehicles

According to GRUNDITZ and EMMA ARFA (2014), vehicle dynamics aims to explain how a vehicle moves on a road surface while being affected by forces between the tyre and the road, gravity, and aerodynamics. The electrical motor, battery, motor drive, battery controller, and vehicle interface make up the bulk of a pure electric car's powertrain. An electric drive system with a battery acting as an energy buffer makes up the power system train of an electric vehicle. The machine is electrically connected to the battery via a DC/AC or DC/DC power electronic converter along with a control system. The battery is where the energy is chemically stored. Figure 3.4 displays the structure diagram of the all-electric vehicle power system. The energy transfer from the battery to the motor and vice versa is turned, respectively, into mechanical and electrical energy.

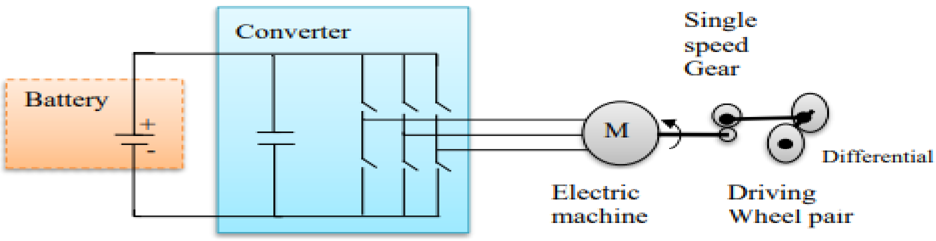

Figure 3. 4: Energy Flow *(Ovidiu, 2012)*

3.4.1. Specification of Three Wheeler Electric Vehicle

As a source of vehicle, the study was used an E-Rickshaw three wheeler for passengers, whose specifications are listed below to analysis the current work with previously done works.

Table 3. 2: Vehicle specification

No	Parameters	Symbols	Values
1	Vehicle mass	M	700 Kg
2	Maximum Power	P	7.25 Kw
3	Wheel Base	B	1318 mm
4	Overall length	L	2625 mm
5	Overall Width	W	1300 mm
6	Overall Height	H	1710 mm
7	Coefficient of Rolling Friction	$C_{r\,r}$	0.015
8	Frontal area	A	2.09 m^2
9	Aerodynamic drag coefficient	C_d	0.44
10	Tyre	R	4.0 * 8.0

3.5. Driving Force and Power of Three Wheeler Electric Vehicle

Road load (B. Tabbache.et.al. 2010) is the sum of the forces that the vehicle must overcome when moving, as indicated in Figure 3.5 below. The aerodynamic drag force Fd, rolling resistance force Fr, acceleration force Fa and clamping (gradient) force Fc make up this road load.

$$F_l = F_r + F_d + F_c + F_a \qquad (4)$$

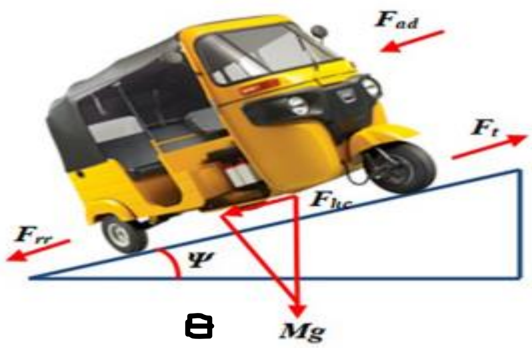

Figure 3. 5: Vehicle Dynamics *(S Devi Vidhya and M Balaji, 2019)*

Assume that there are 4 total passengers, the vehicle is travelling at 65 km/h, or 18 m/s, the wind component is at 3 m/s, and the average weight of each passenger is 65 kg. Total Passenger Weight = 4 x 65 = 260 kg as a result. Assume that the motor weighs 50 kg, the hull weighs 100 kg, and the battery weighs 290 kg. The total weight of the passengers, the weight of the battery, the weight of the hull, and the weight of the motor may all be added to determine the mass of the vehicle, or Mv, which is equal to 260 + 290 + 50 + 100 = 700 kg. Considering the power requested for starting speed of 15km/h the angle of gradient was $\Theta = 6^{o}$ (10%), the air density is 1.225 kg/m3 and that the gravitational acceleration is g = 9.81 m/s2.

3.5.1. Rolling Resistance

According to Chauhan (2015), rolling resistance is the force that prevents a vehicle's wheels from rolling as a result of non-elastic phenomena at the tire-road surface.

Table 3. 3: Values of Rolling Coefficient

Rolling resistance coefficient values for many types of roads

Contact surface	$C_{r\,r}$
Concrete(good/fair/poor)	0.010/0.015/0.020
Asphalt(good/fair/poor)	0.012/0.017/0.022
Macadam(good/fair/poor)	0.015/0.022/0.037
Snow (2 inch/4 inch)	0.025/0.037
Dirt(smooth/sandy)	0.025/0.037
Mud(firm/medium/soft)	0.037/0.090/0.150
Grass(firm/soft)	0.055/0.075
Sand(firm/soft/dune)	0.060/0.150/0.300

Rolling resistance is computed using the following formula:

$$F_r = C_{r\,r} \times M \times g \times \cos(\Theta) \qquad (5)$$

$$= 700 \times 9.81 \times 0.015 \times \cos(6^{0}) = 102.44 \text{ N}$$

Where, Cr r: Coefficient of rolling resistance, and (mxg): Vehicle weight in N and Θ inclination angle. The Power needed to overcome the N's rolling resistance is:

$$P_r = F_r \times V \text{ (m/s)} \qquad (6)$$

$$= 102.44 \times (65 \text{ Km/hr}) = 1.84 \text{ KW}$$

3.5.2. Force of Aerodynamic Drag

When a vehicle is moving through the air, an aerodynamic drag force is exerted on the body of the vehicle. It has three parts: induced drag (caused by trailing vortices), normal pressure drags (dependent on vehicle frontal area and speed), and skin friction drags (caused by air flow in the boundary layer). Surface irregularities of the roads tend to change the speed of light vehicles such as three wheelers during coast-down test. These speed variations create significant changes to the calculation of aerodynamic drag coefficient and rolling resistance by the methods to found aerodynamic and rolling coefficient (J.A.K.S.Jayasinghe,B.S. et. al, 2009). The following gives the expression for aerodynamic drag:

$$F_d = 1/2 \text{ x} V^2 \text{ x } C_{d \text{ x}} \text{ A x } \rho \quad (7)$$

$$= ½ \text{ x } 1.23 \text{ x } 0.5336 \text{ x } (18 + 3)^2 = 144.72 \text{ N}$$

Where V is the total speed of the vehicle plus the speed of the air, measured in m/s, and Cd is the aerodynamic drag coefficient. In general, ρ is assumed to be 1.23 Kg/m3, Cd ranges from 0.2 to 1.5, and A is the frontal area of the plate shape, which is equal to 0.58 x 0.92, or 0.5336 m2. And the following expression can be used to compute Cd: $C_d = Fa/0.5\ \rho AV^2$.

The aerodynamic drag power is given by: where $V_d = V_{max} /2$

$$P_d = F_d \text{ x } V_d \text{ (m/s)} \quad (8)$$

$$= 144.72 \text{ x } 65/2 \text{ (Km/hr)} = 1.3 \text{ KW}$$

3.5.3. Gradient Resistance Force

Gravitational force manifests itself as gradient resistance. It is the force that, while a vehicle is climbing an inclined surface, tends to pull the vehicle back. The vehicle's grade resistance can be determined as follows:

$$F_g = \text{M x g x sin } (\Theta) \quad (9)$$

$$= 700 \text{ x } 9.81 \text{ x sin } (6^0) = 717.79 \text{ N}$$

And Pg = Fg x Vg provides the Bajaj's climbing capacity. Where, we assume that

For 15km/h $\Theta = 6^0$ incase of gradient and Vmax /2 (m/s) represents the climbing speed.

$$P_g = F_g \text{ x } V_g \quad (10)$$

= 717.79 x 15/2 Km/hr = 1.5 KW

The sum of rolling resistance, aerodynamic drag, and grading resistance, or total resistive force, is thus calculated.

$F_{total\ resistive} = F_r + F_d + F_g = 102.44 + 144.2 + 717.79 = 964.43$ N

And Total tractive power is:

$P_{total\ tractive} = P_r + P_d + P_g = 1.8 + 1.3 + 1.5 = 4.6$ KW

Assume transmission efficiency be 0.86 radius of wheel R_w= 0.4 and gear ratio 3.5 then mechanical power or rated output power is defined as:

$P_{mech} = P_{total\ tractive/\eta}$ (11)

= 4.6/0.86 = 5.35 KW

Vehicle speed in revolution per minute is:

V (rpm) = V_v(m/s) x 60 /2πR_w (12)

= 18 x 60 /2x π x 0.4 = 429.7 rpm

The motor's rated speed is then determined as follows:

N_m = V (rpm) x gear ratio (13)

= 429.7 x 3.5 = 1500 rpm

Maximum Torque produced = $P_{mech\ x\ 60}$ /2π N_m (14)

= 5.35 x 60 /2 π x 1500 = 34 N-m

Table 3. 4: Specification of PMDC motor

Parameters	Value
Rated Power	5 KW
Specified Voltage	350 V
Maximum Current	54 A
Rated Speed	1500 rpm
Efficiency	83%

3.5.4. Selection of Electric Vehicle Battery

Batteries serve as the pure electric vehicles' power source. The selection of battery specifications must take into account the need for maximum driving power and endurance mileage requirements. Since lithium ion batteries have a high mass energy density and a long life, they are chosen as the power source for electric vehicles. In literature, stated that efficiency, energy density, and criteria for cost, runtime, durability, and safety are all important considerations (Lu L., Han X., Li J., Hua J., and Ouyang M., 2012). For this thesis, the chosen battery was lithium-ion batteries. DC power for EVs can be stored in the lithium battery pack.

Batteries are a vital part of green technology and the mainstay of electric vehicles. The types of batteries utilised have a significant impact on how well an electric car performs. However, the electric vehicle battery is prone to overheating. To avoid such issues, the EV must have a coolant device on its hood and must be shut off throughout the charging process. The battery is also the primary cause of the electric vehicle's exorbitant price. Many dry cell batteries that we have used in our daily lives make up the battery pack in an electric vehicle.

The lithium battery packs are made up of serially arranged conventional lithium battery modules. Each battery module can store 4kWh. For the suggested EV, a battery pack with a total power of more than 35kWh and a rated DC voltage of 48V that is serially coupled from more than eight battery modules is needed. In order to meet the demand for total energy, there are four battery modules that are serially coupled. As a result, the choice of battery specifications must take into account both the vehicle's maximum power and the desire for endurance miles (X. Xin and C. Zhang, 2017).

$P = P_{max} \times 0.15 + 0.85 \times P$ (@zero grade and constant speed) (15)

$P_m = P/\eta_m$ (16)

$W_{road} = P_{m \times t} = P_{m \times S/V}$ (17)

$SOC = (W_{rated} - W_{road}) / W_{rated} \times 100$ (18)

Where Pm is the input power of the motor drive, ηm is the efficiency of the motor and motor controller assembly, S is the endurance mileage, Wrated is the energy needed for mileage S, and P is the power necessary for the car at constant speed, P.

3.5.5. Battery Pack

When modelling the battery electric vehicle (BEV), an estimation of the battery pack size was helpful. The battery size was determined by multiplying the energy consumption by the car's range, then dividing that result by the battery's specific energy. For predicting battery behaviour in various operating scenarios, calculating battery death from discharge, state of charge (SOC), state of health (SOH), and remaining battery life, a suitable lithium-ion battery model is required (Bobba PB and Rajagopal KR, 2012).

A Li-ion model based on an equivalent electrical circuit is shown in Figure 3.6. The battery's open-circuit voltage, V_{OCV}, and a series resistor, R_O, which stands in for the ohm resistance drop, make up this analogous circuit model. The parallel RC branch accounts for the diffusion charge, with Vt being the terminal voltage of the battery as measured across its terminals, given by; Diffusive resistance is represented by R_1 and R_2, while diffusive capacitance is represented by C_1 and C_2.

$V_t = V_{OCV} - V_1 - V_2 - V_3$ (19)

The integral equation is used to compute the battery's SOC.

$SOC_t = SOC_{initial} - 1/3600 \int_{to}^{t} ibattery\ (t)dt$ (20)

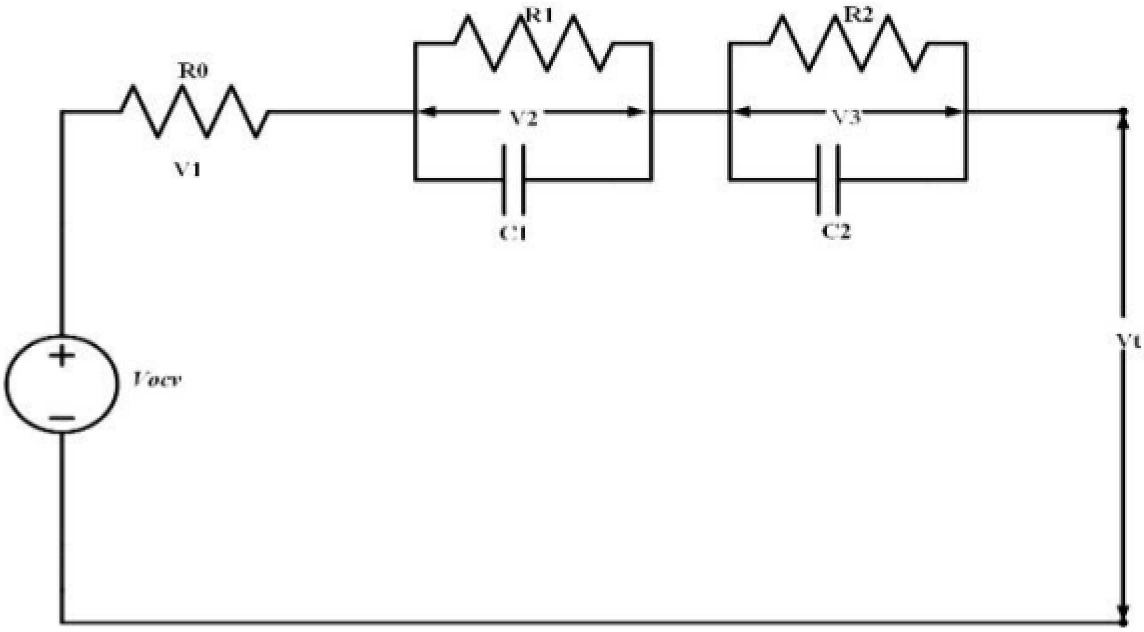

Figure 3. 6: Equivalent Circuit based Li-Ion Battery *(Sudhansu, 2022)*

SOCinitial is the condition of charge when the vehicle is first started, where SOCt is the state of charge at a time, or "t," Direct power from the battery pack, which has a terminal voltage of 48 V, is used to drive the motor. A SOC of 20% to 100% is estimated to be sufficient for the battery to operate. A BES system reduces the energy required from the battery to 220.98N, or 4 kWh, for a maximum range of 75 km (S Devi Vidhya and M Balaji, 2019). In order to store 4 kWh of energy for up to 75km of range per charge, 520 cells (40 stacks of batteries with 13 cells in series) are needed.

Table 3. 5: Specification of Vehicle Battery

Parameters	Values
Cell type	Lithium-Ion
Total Battery Power Pack	7.37 KWh
Rated DC Power Supply	350 V
Ah rating	90 Ah
Mass	32 kg
Nominal Voltage	12 V
Energy Density	154 Wh/kg
Operating Temperature	-10 ℃ to 50 ℃
Energy	4800 Wh

3.6. Design of three wheeler electric vehicle Chassis Frame

The four main loading scenarios that the chassis typically encounters are vertical bending, longitudinal torsion, lateral bending, and horizontal lozenging. When the tricycle's equipment, passengers, and luggage are placed in the centre of the wheel base of the chassis frame, which is supported at its ends by the wheel axles, the side members droop in the middle.

3.6.1. Calculation for Reaction Forces

Calculations in general for the load on the chassis frame

- ✓ Gross vehicle weight = 700 kg
- ✓ Curb weight of the vehicle = 346 kg
- ✓ Total load to be applied = 700x9.81 = 6867 N
- ✓ Considering an overload of 20% of the total load = 6867x1.2 = 8240.4 N
- ✓ The chassis structure is made up of two pieces, therefore each side component is subjected to half of the overall stress.
- ✓ Load on a single frame = 8240.4/2 = 4120.2 N/member

The chassis is merely a clamp with a coil spring and shock absorber, making it a simple supported beam with even load distribution.

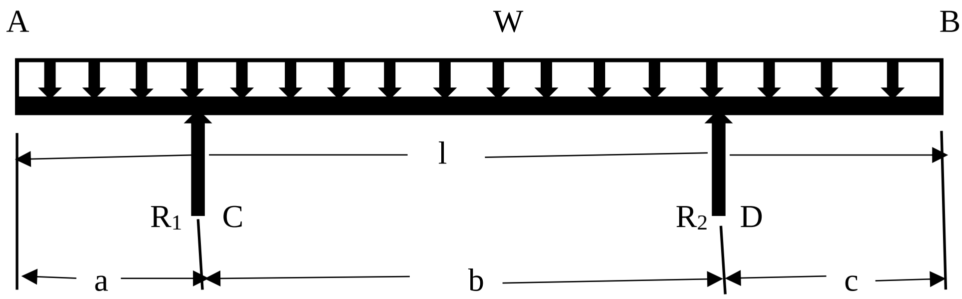

Figure 3. 7: Chassis frame as simply supported beam with over hung

The total load acting on the beam's span is 4120.2 N, the beam’s length is 2010 mm. The load that is currently evenly distributed is w = 4120.2N/2010 mm equals 2.05 N/mm, l is 2010 mm, front overhangs a and b are 251 mm and c is 125 mm, respectively. Then considering the response to support A:

$$R_C + R_D = 4120.2 \text{ N} \quad (21)$$

$$R_C = wl\,(l - 2c)/2b \quad (22)$$

Where RC denotes the reaction force at point C, w denotes the distributed load across the member, l denotes the length of the side member, and a, b, and c denote the distances between A, B, C, and D.

$\therefore$ R_C = 2.05N/mm x 2010 mm (2010 mm – 2 x 125 mm)/2x1634 mm = 2219.12 N

From equation (16): $R_C + R_D$ = 4120.2 N

R_D = 4120.2 N – 2219.12 N = 1901.08 N

3.6.2. Calculation for Shear Forces

The shear forces and bending moments of the chassis frame are calculated as the following equations:

$\tau_A = w \times a$ (23)

= 2.05 N/mm x 251 mm = 1068.05 N

$\tau_B = w \times c$ (24)

= 2.05 N/mm x 125mm = 256.25 N

$\tau_C = R_C - \tau_A$ (25)

= 2219.12 N – 1068.05 N = 1151.07 N

$\tau_D = R_D - \tau_B$ (26)

= 1901.08 N – 256.25 N = 1644.83 N

3.6.3. Calculation for Bending Moment

$M_{left} = - w a^2$ (27)

= - 2.05 x $(251)^2$ /2 = - 64576.025 Nmm

$M_{right} = w c^2 /2$ (28)

= - 2.05 x $(125)^2$ /2 = - 16015.625 Nmm

$M_{mid} = R_C ((R_C/2w) – a)$ (29)

= 2219.12 ((2219.12/2 x 2.05) - 251) = 644096.87 Nmm

3.6.4. Calculation for Stress Generated

From the above calculation the maximum bending moment is 644096.87 Nmm, from this value the deflection can be calculated as equation below. Square cross section 40mm x 40mm x 3mm.

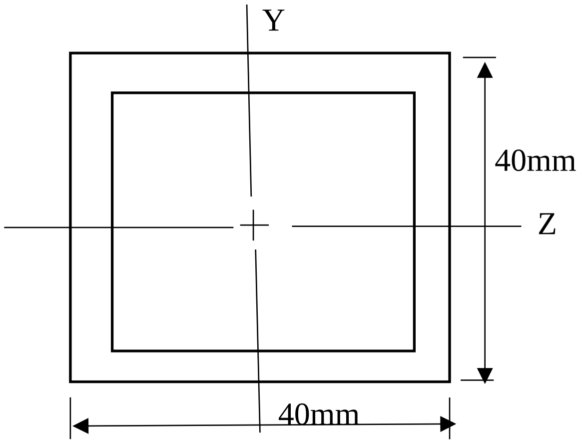

Figure 3. 8: Cross section for the chassis frame

Moment of inertia along the z-z axis is:

$I_Z = (bh^3 - b_1h_1^3)/12$ (30)

$= 40mm \times (40mm)^3/12 - 34mm \times (34mm)^3/12 = 101972mm^4$

The deflection of chassis frame is calculated by driving equations from different equations of the theory of ductile materials. The top peripheral of the cross section, i.e., y=20mm, has the highest compressive stress, whereas the bottom periphery, i.e., y = -20mm, experiences the highest tensile stresses. By using the largest bending moment, an analytical computation can determine the bending moment for a particular cross section of a side member ladder frame.

$M/I = \sigma/_\gamma = E/R, \quad \sigma = \pm M \times Y/ IZ$ (31)

Where y is the stress at a distance from the N.A. (z-z axis) of the beam cross-section, M is the bending moment, Iz is the second moment of area, and σ is the stress.

$\sigma = \pm M \times Y / IZ = \pm 644096.87 \times 20 / 101972 = \pm 126.33$ MPa

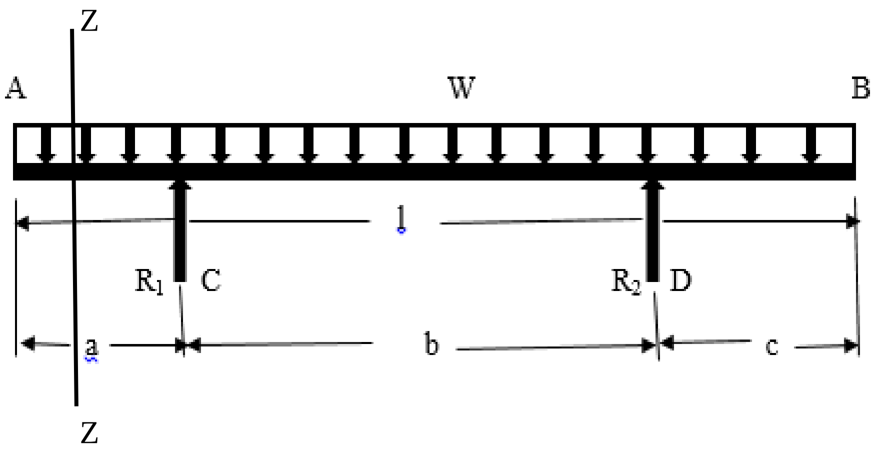

Figure 3. 9: section z-z of chassis beam

Finding the instant at z-z, considering clockwise motion as favourable,

$M_{Z\text{-}Z}$ =-2.05N/mm x (2010-x)-R_C x (x-1759)-R_D x (x-125) +2.05N/mm x (x/2) (32)

= -2.05N/mm x (2010mm-$x$mm) – 2219.12N x ($x$mm – 1759mm) – 1901.08N x (x/2)

= 3899311.58 – 3167.67 x

However, the following equation provides the bending moment:

$M = Eid^2y / d^2x$ (33)

Slope is discovered by integrating this equation.

$\Theta = dy/dx$, $\sigma = y$ (34)

The deflection (σ) of the beam is obtained from the second integration of this equation. The following deflection equation throughout the length of the beam is then produced by twice integrating the bending moment equation from above.

EI σ = -527.95 x 3 + 1949655.79 x 2 + AX + B

Where the boundary conditions must be used to solve for the integrating constants A and B.

When x = 125 and 1759, respectively, y = 0, the values of A and B are A = -19.15 x 10^8 and 20.99 x 10^{10}, respectively, and EI = 200 x 10^3 x 101972, or 20394400000Nmm2.

When these numbers are substituted in the equation for deflection, the maximum deflection is found at the intersection of supports C and D at x = 1068mm.

$EI\sigma_{max} = -527.95(1068)^3 + 1949655.79(1068)^2 – 1915299219.41(1068) + 209980183051.25$

$20394400000\sigma_{max} = -254876724240.07$

$\sigma_{max} = -12.49mm$. According to this outcome, the distortion is 12.49mm downward.

3.7. Solid works modelling of the chassis for a three-wheeled electric vehicle

The 2D and 3D Chassis frame model created by solid work software is shown in figure below.

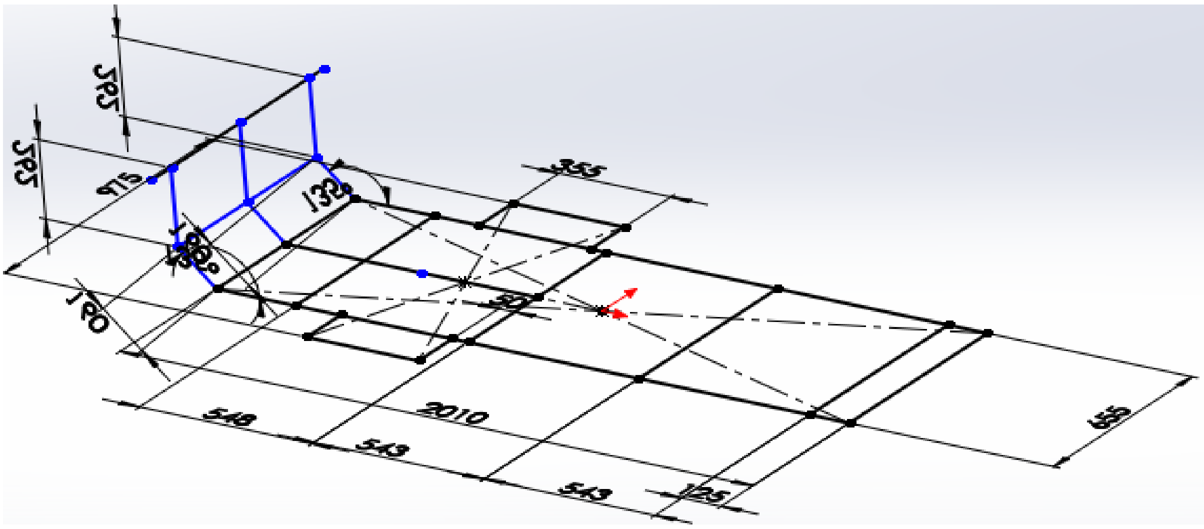

Figure 3. 10: 2D drawing of Three Wheeler vehicle Chassis frame

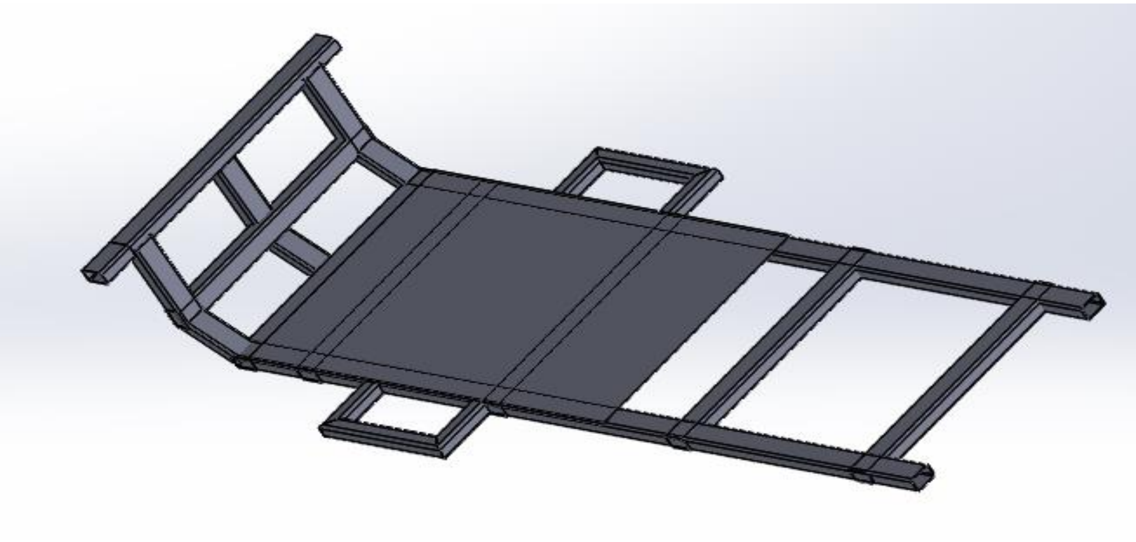

Figure 3. 11:3D Model of three wheeler electric vehicle

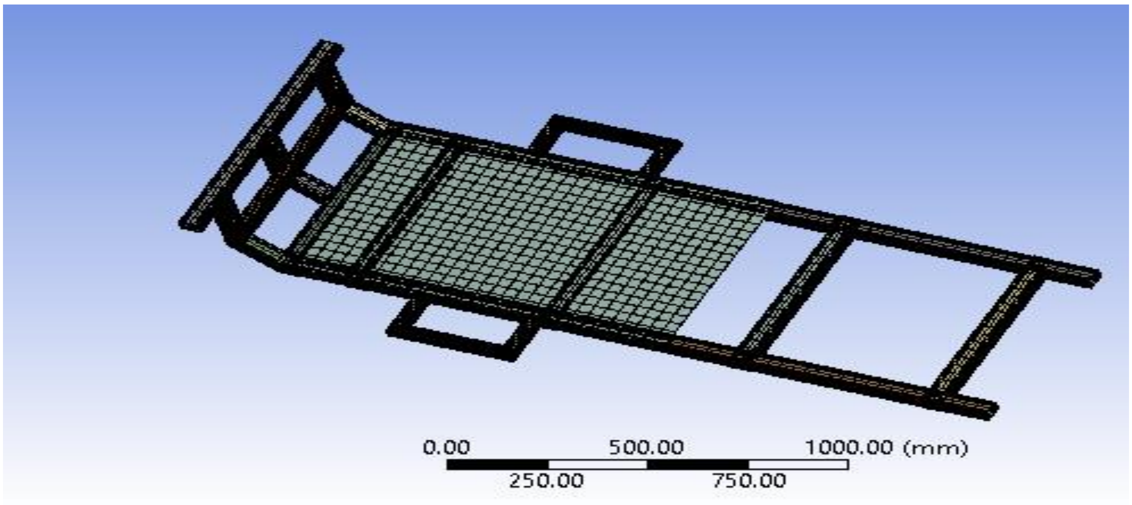

Figure 3. 12*:* Three-wheeled electric vehicle chassis frame with mesh design

3.8. Matlab-Simulink Modelling of electric vehicle

In Matlab 2019a, the desired battery electric vehicle (BEV) model was created. For ease of use, the wind speed (Vwind) and road angle (ϴ) were set to zero during the Matlab simulation. A driving cycle is the simulation model's input, and the model's output is all of the vehicle's distance, speed, charge level, current, voltage, etc. Here are the block sets from the Matlab/Simscape software that were used to simulate the necessary electric vehicle along with a screen shot.

3.8.1. Drive Cycle Source

The drive cycle source generates a standard or user specified longitudinal drive cycle. The block output is the vehicle longitudinal reference speed as a function of time, along with gear shift schedule if applicable. It is used to produce realistic velocity and shift schedules for closed loop acceleration and braking commands for vehicle control and plant modules. Figure 3.13 below displays the physical modelling of the drive cycle as extracted from the Simscape block diagram. The vehicle reference speed of the longitudinal driver is connected to the reference speed port of the drive cycle.

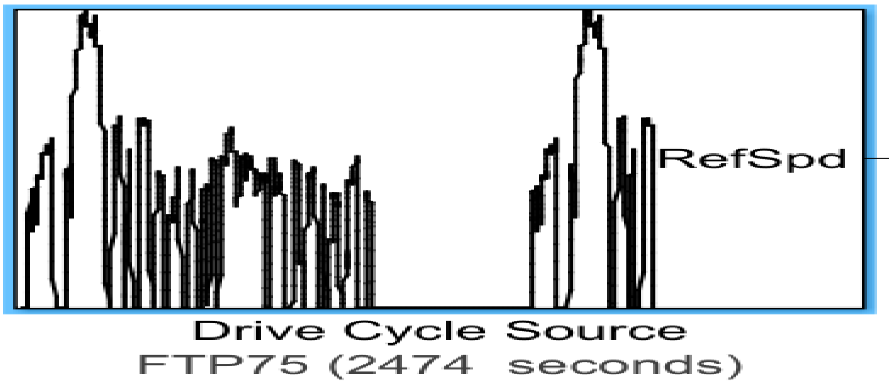

Figure 3. 13: Drive Cycle Source

3.8.2. Longitudinal drive

The longitudinal driver block implements a longitudinal speed tracking controller. Based on reference and feedback velocities the block generates normalized acceleration and braking commands that can vary from 0 through 1. The longitudinal driver controls the vehicle's speed by accelerating and decelerating, as depicted in Figure 3.14 below.

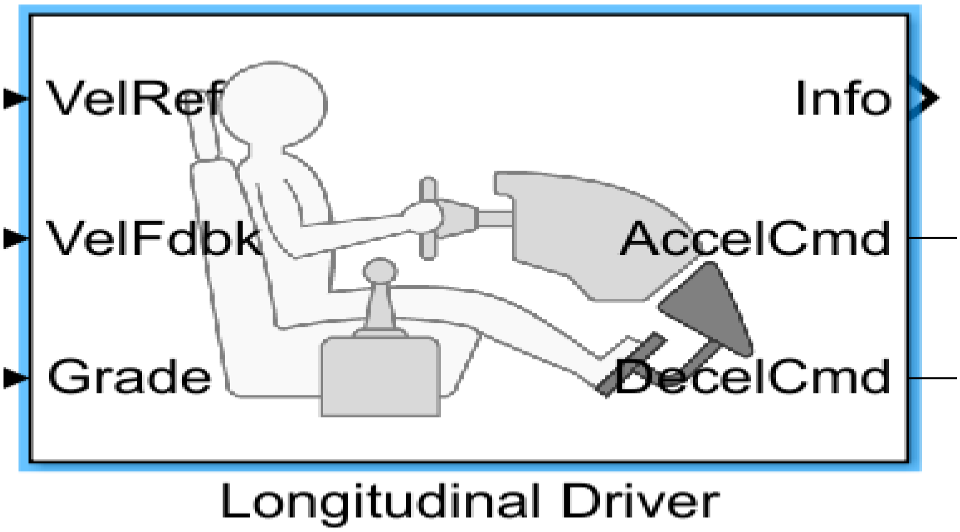

Figure 3. 14: Longitudinal Driver

Where:

VelRef = Vehicle reference

VelFdbk = Vehicle feedback

AcelCmd = Accelerator command

DecelCmd = Decelerator Command

3.8.3. Electric Motor and Controller Subsystem

The tractive force required to drive the vehicle is obtained from PMDC motor. The torque-speed characteristics of the motor are used to obtain tractive force at given vehicle load and floor conditions. The H-bridge motor drive block can be driven by the controlled PWM .In PWM mode the motor is powered if the PWM port voltage is above the enable threshold voltage. The physical model created by Matlab-simulink and Simscape for this thesis' PMDC electric motor is displayed in Figure 3.15 below. The motor's rotor (R) is coupled to the input shaft of the gearbox, and the C port is grounded to the mechanical rotational reference.

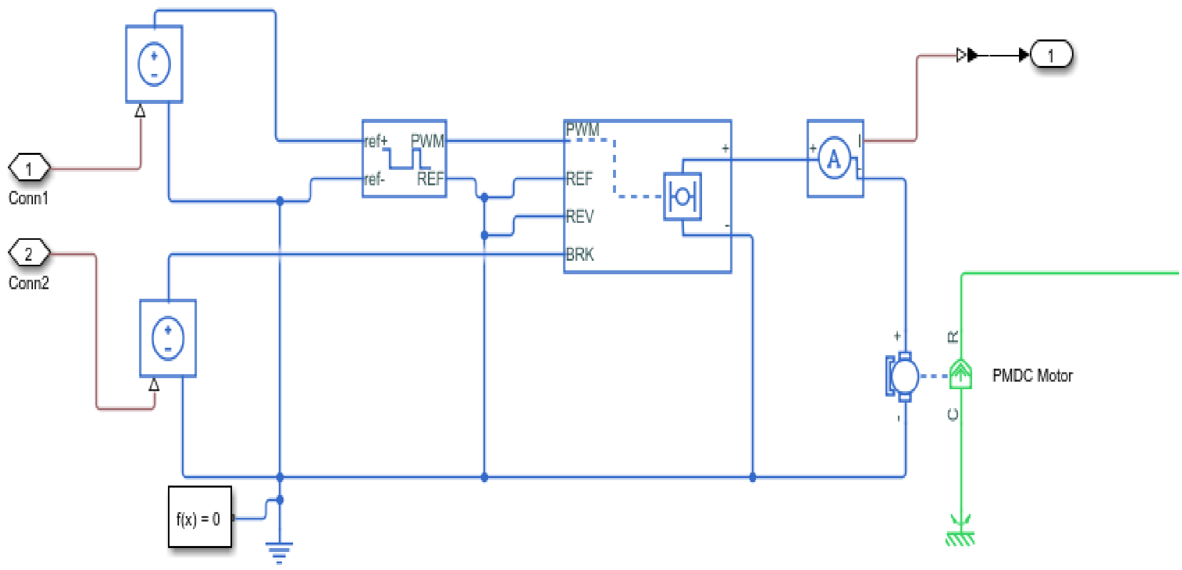

Figure 3. 15: PMDC Motor and Controller

3.8.4. Battery and Battery Pack Subsystem

The electric car's engine is its battery pack. It is made up of an association of constituent cells in series or parallel. Starting with the battery cell, the Matlab/Simscape software models the whole battery pack structure.

Figure 3.16 below shows the electrical circuit diagram for a battery cell. Resistors and a dc voltage source are present. The nominal voltage of each cell is 3.6 volts. Poor range performance results from an increase in battery voltage caused by connecting battery cells in series while maintaining a consistent Ah capacity. The battery capacity (Ah) improves when battery cells are coupled in parallel, which results in a good operating range.

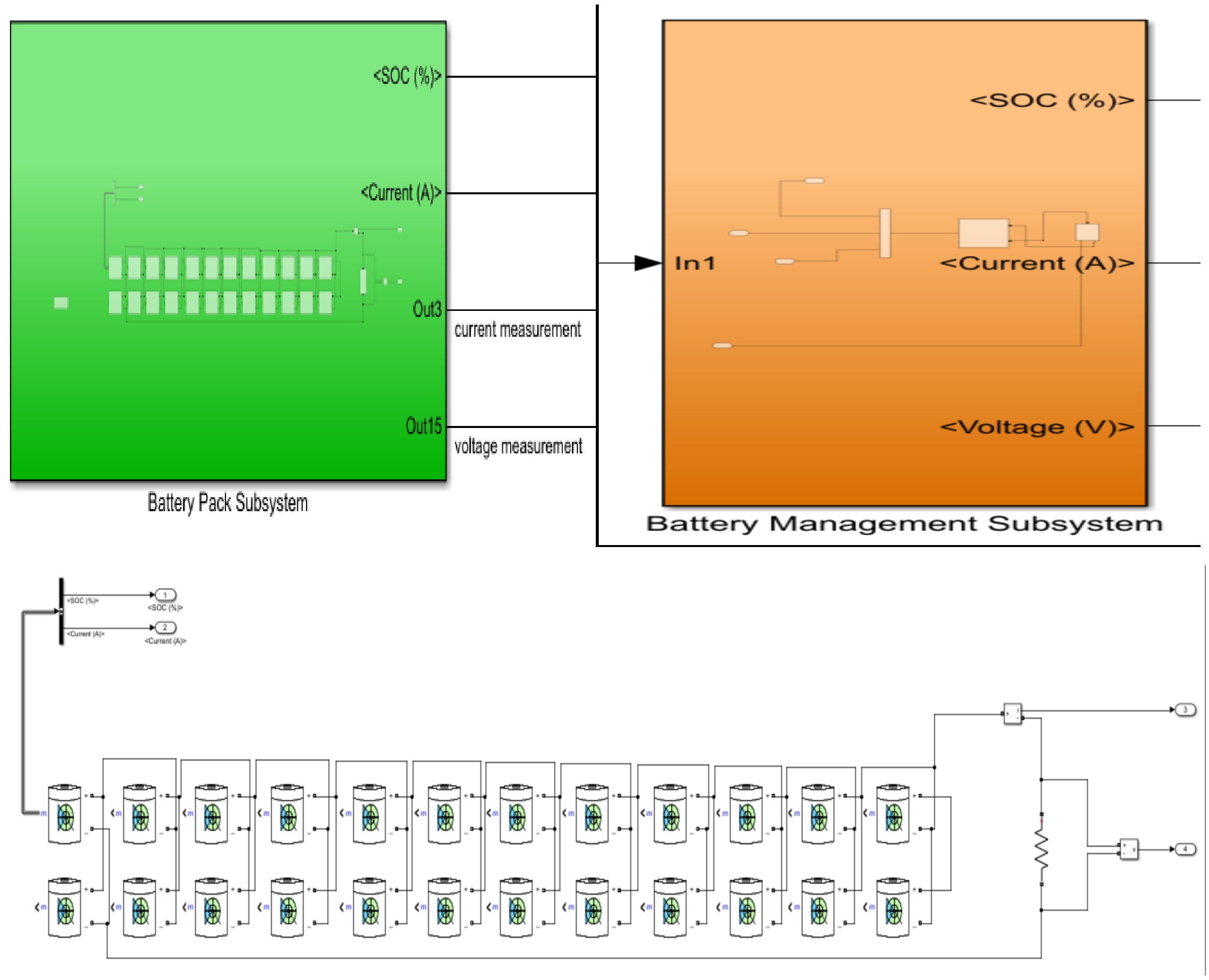

Figure 3. 16 Battery cells and pack

3.8.5. Vehicle body, tyre and gearbox

Figure 3.17 below depicts the physical modelling of a straightforward gearbox, gearbox and tyre that was extracted from Simscape. The tire block is built from tire-road interaction, simscape foundation library wheel and axle blocks. The left and right wheels are linked to the gear box output shaft (F) port and the rotor shaft of the PMDC motor is attached to the gear box input shaft (B) port.

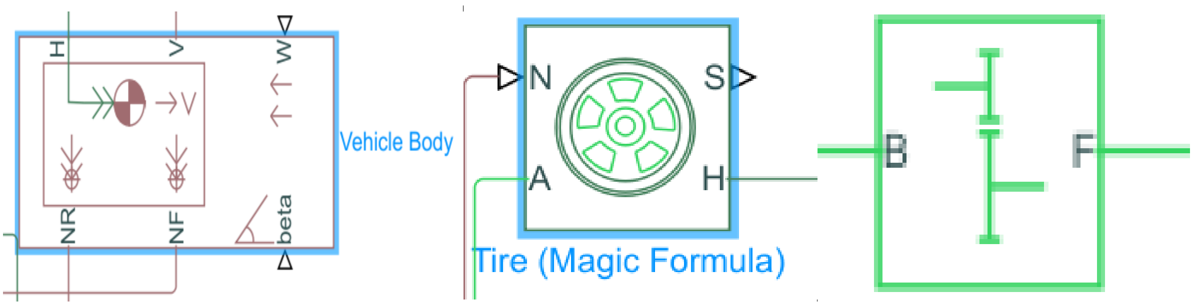

Figure 3. 17: Vehicle body and tire

3.8.6. Vehicle Body Subsystem

Figure 3.18 below depicts the vehicle body, which was obtained from Simscape's physical modelling. In addition to being used to supply vehicle dynamics parameters, it has ports for velocity, wind, slope, wheel hub, and front and rear normal forces.

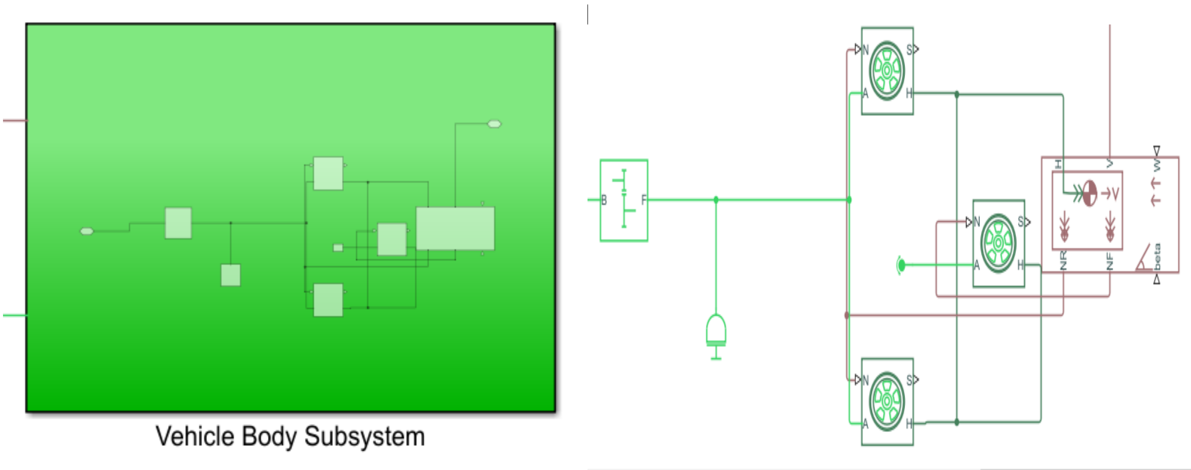

Figure 3. 18: Vehicle Body subsystem

3.8.7. Overall Modelling System

The complete model of the thesis consists the vehicle body subsystem, motor and its controller subsystem, battery subsystem and drive cycle source is shown in figure 3.19.

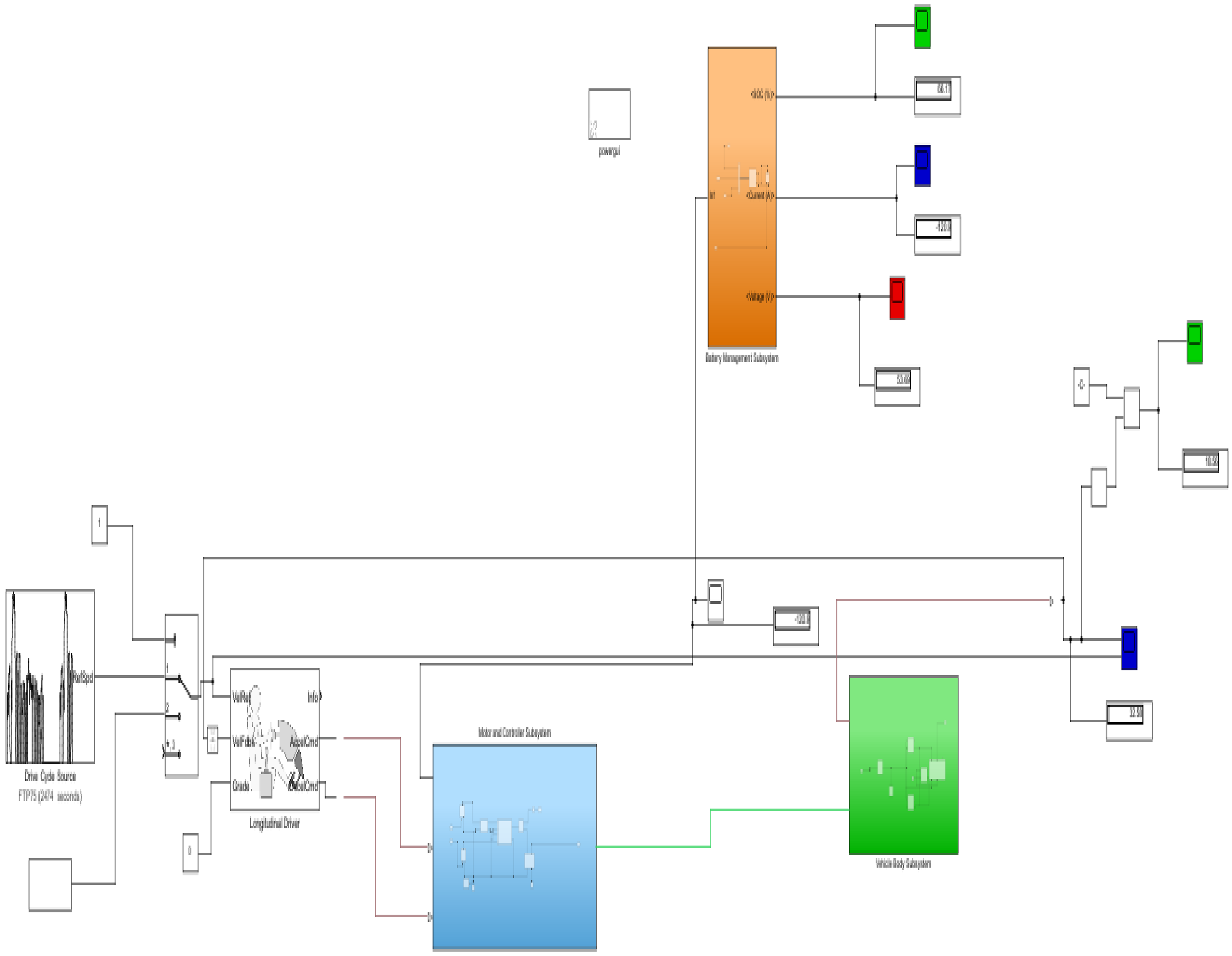

Figure 3. 19: Overall Vehicle Model

CHAPTER FOUR

RESULTS AND DISCUSSION

4.1. A Three Wheeler Electric Vehicle Chassis Frame Analysis

4.1.1. Analysis Using Finite Elements

The stress and modal analysis of the electric vehicle chassis is the primary goal of the finite element analysis. Various analyses include:

- ❖ The Modal Analysis:
- ➢ Discover the chassis' mode forms for the first six natural frequencies.
- ➢ frequency of resonance
- ❖ Analysis of Harmonics :
- ➢ Plotting the amplitude vs. frequency graph to determine the resonance frequency for the chassis.
- ❖ Analysing Static Structure:
- ➢ Finding the place of the maximum deflection

4.1.2. Three-wheeled electric vehicle chassis frame modal analysis

Natural frequencies and mode shapes can be found via a modal analysis utilising the finite element method. Modal analysis for this investigation was carried out using the finite element programme ANSYS 16. The first six frequencies in the global vibration, which play a significant role in the dynamic behaviour of the chassis, have been examined after creating a finite element model of the chassis and using the proper meshing.

The physical model is often represented using a CAD model using FEA software, which then divides it into tiny bits known as finite "elements." "Meshing" refers to this procedure. The mathematical representation of the physical model was improved by a mesh (collection of elements) of higher quality. Using small pieces, the mesh is created for the model.

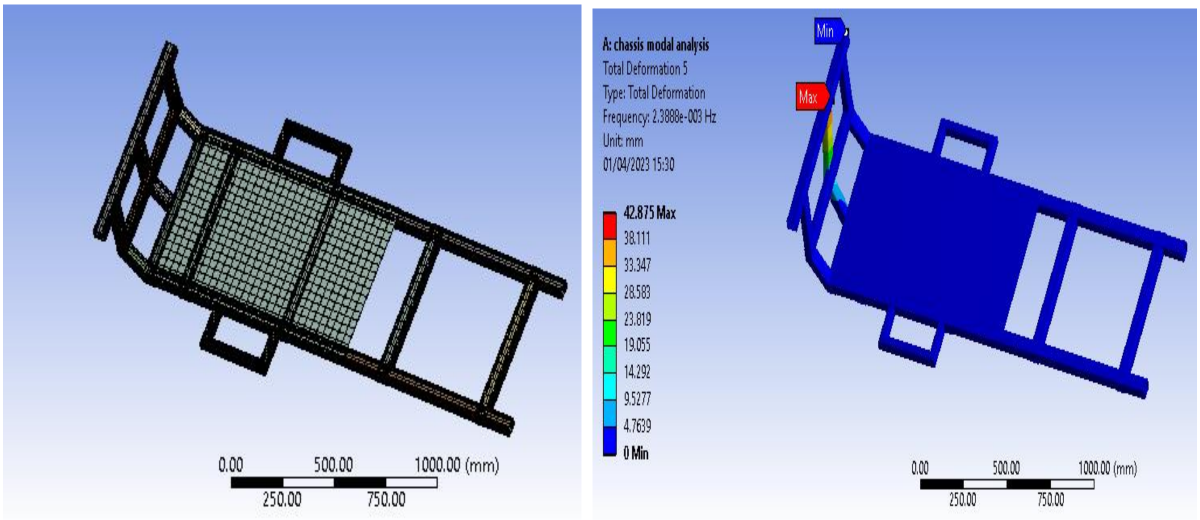

Figure 4. 1: Meshed and modal analysis of three wheeler electric vehicle chassis frame

Before importing, it is expected that the member is completely linked. Solidworks 2015 is used to generate a streamlined CAD model of the planned electric vehicle frame, which is then imported as an external geometry file into ANSYS 16.0.

Table 4. 1: Modal Analysis of three wheeler electric vehicle chassis frame

<table>
<tr>
<td>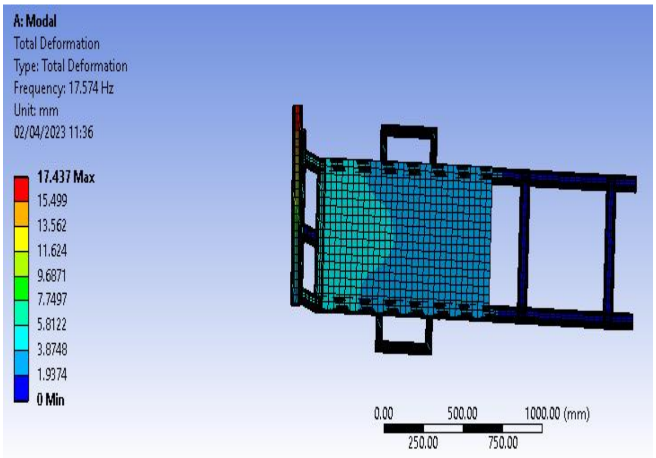

With a total deformation of 17.437mm, the initial global mode shape of the electric car chassis frame is at 17.574 Hz. The chassis moved upward and downward. The front top of the vehicle's chassis saw the greatest translation.</td>
<td>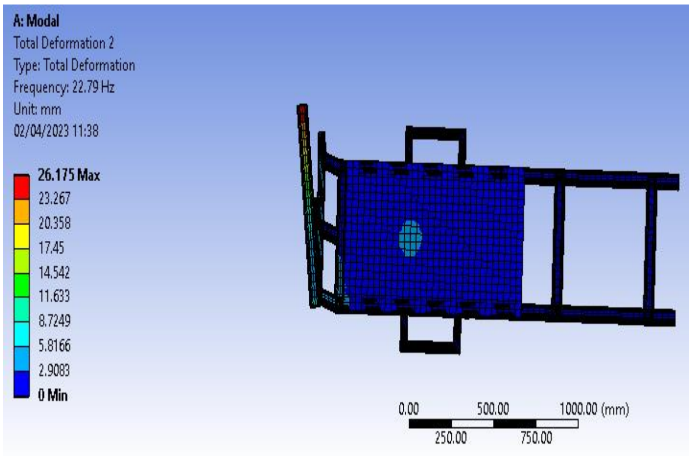

The second global mode shape of the electric vehicle chassis at a total deflection of 26.175mm at a frequency of 22.79Hz. The chassis moved to the front and the back. The front top corner of the vehicle's chassis experienced the greatest translation.</td>
</tr>
</table>

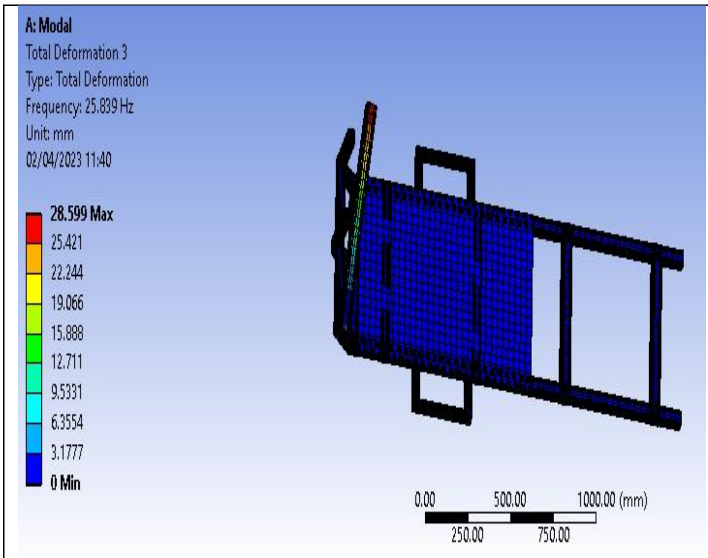

The third global mode shape, with a 28.599mm deflection, of the electric vehicle chassis. The Front top part modes were experienced by the chassis. The area of the car chassis with the greatest translation was on the right.

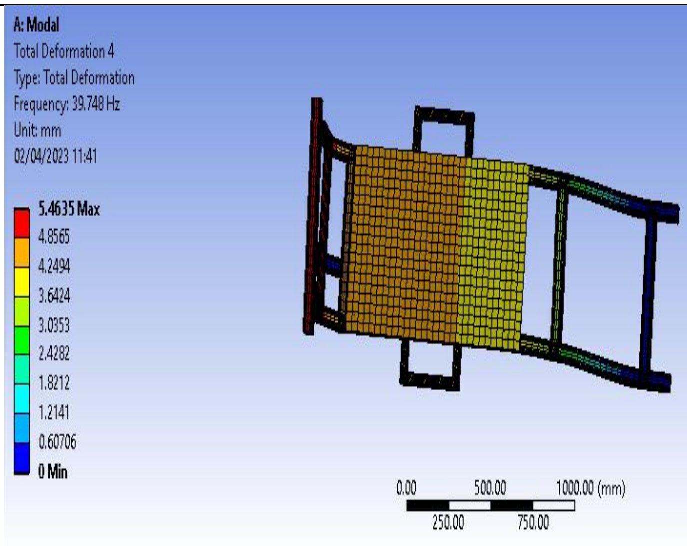

The electric vehicle chassis’ fourth global mode shape vibrates at a frequency of 39.748 Hz and deforms by 5.4635 mm. The chassis went through a Z-axis bending mode. The middle of the chassis had the most translation.

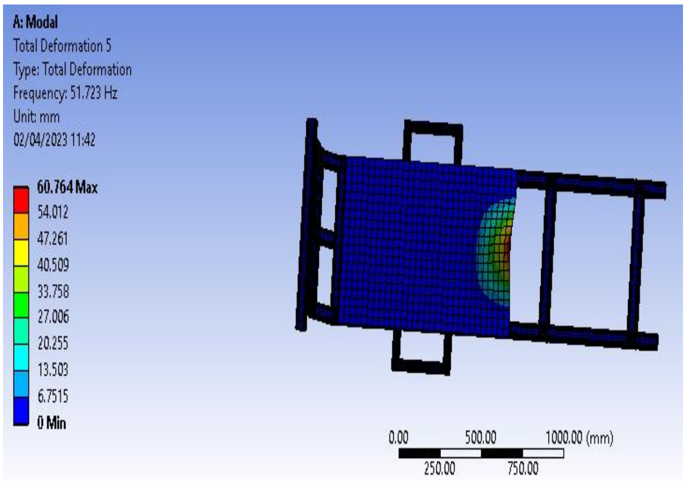

The electric car chassis' Fifth global mode shape at 51.723 Hz. The midsection of the chassis experienced buckling. The metal sheet of the vehicle chassis’ midsection had the greatest translation.

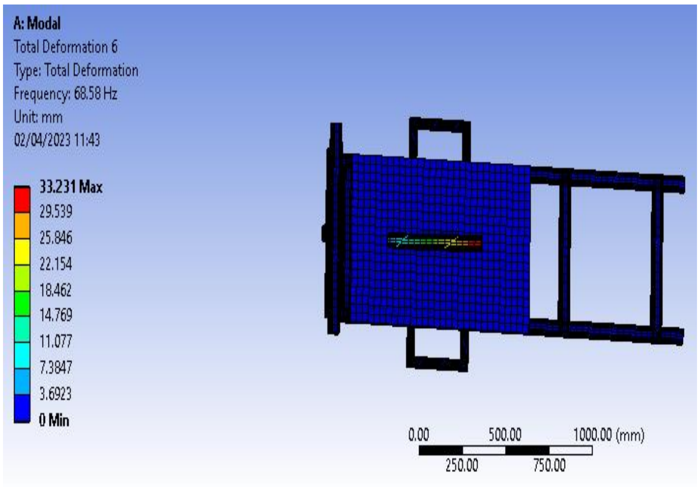

The electric car chassis' sixth global mode shape at 68.58 Hz. The chassis went through a Z-direction twisting mode. The centre of the vehicle chassis' supporting frame was where the maximum translation occurred.

The frequency at each calculated mode is shown in the following bar chart and tabular data.

Tabular Data

	Mode	Frequency [Hz]
1	1.	17.574
2	2.	22.79
3	3.	25.839
4	4.	39.748
5	5.	51.723
6	6.	68.58

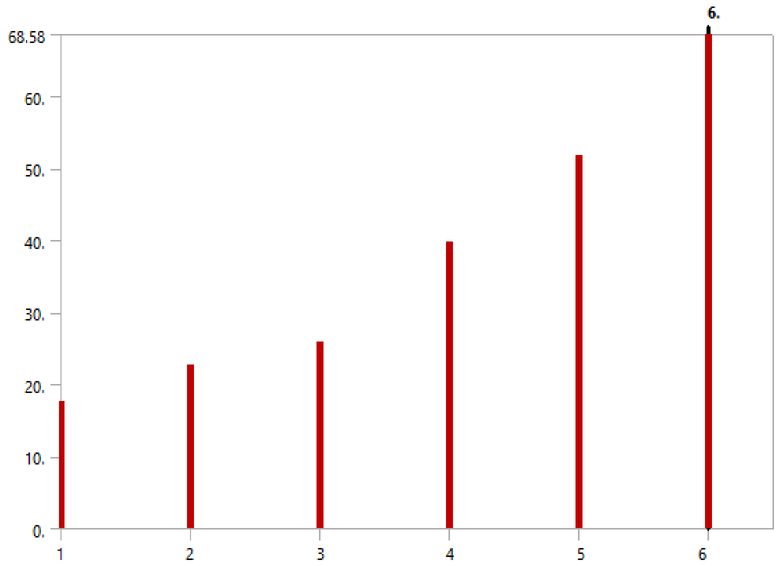

Figure 4. 2: Chart of the frequency for modal analysis

4.1.3. Three-wheeled electric vehicle chassis frame harmonic analysis

The steady-state response of a linear structure is verified using the results of harmonic analyses, allowing researchers, engineers, and chassis designers to decide whether the chassis can tolerate resonance, fatigue, or other structural issues caused by vibration throughout its operational life. A structure's reaction to cyclic loads over a variety of frequencies is calculated using harmonic analysis, and the response is then plotted on an amplitude versus frequency graph.

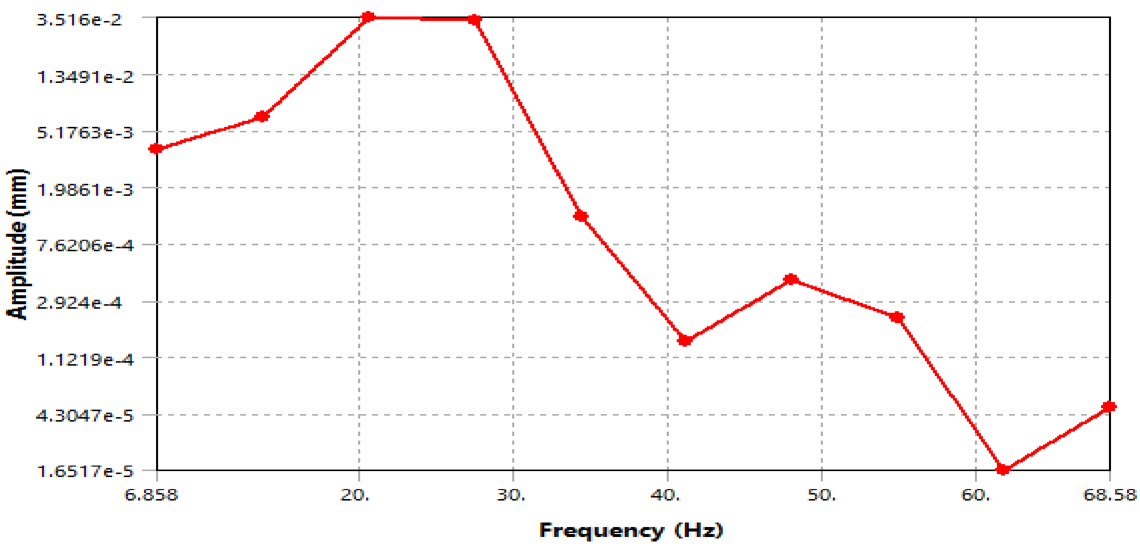

Figure 4. 3: Frequency Amplitude for Harmonic analysis

The lowest observed amplitude of 0.16517 mm at about 60 Hz is shown in Fig. 4.3 above. The frequency at the plot's highest peak amplitude corresponds to the sixth mode shape frequency of the car's chassis. As it was inferred from the analysis the chassis frame modelled was enough safe for the calculated load to get the desired vehicle performance, except at certain frequency mode the more vibration of the vehicle the more it cause the chassis frame distortion.

4. 2. Matlab Simulation Results

The simulation used in this chapter produced the same values of the system parameters that were being investigated. The simulation was carried out to verify how well electric vehicles performed under the specified conditions. The simulation findings were compared to those of previously utilised vehicles, and it was discovered that the performance characteristic had significantly improved.

4.2.1. Vehicle speed Analysis

The curve for the Drive cycle input for both the reference speed and the vehicle speed is shown in the simulation that follows.

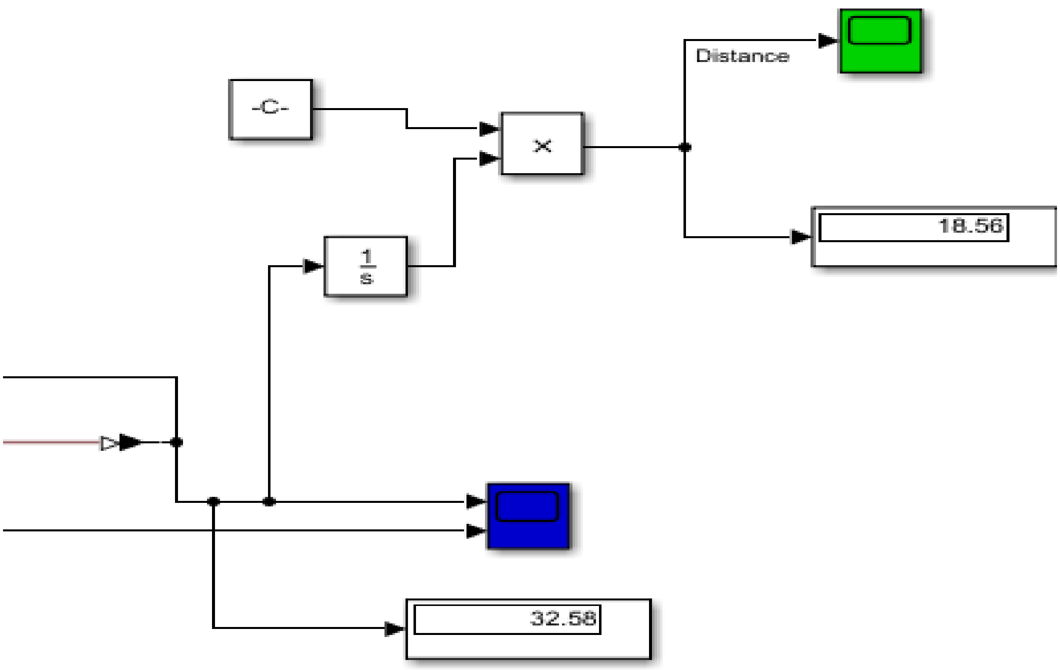

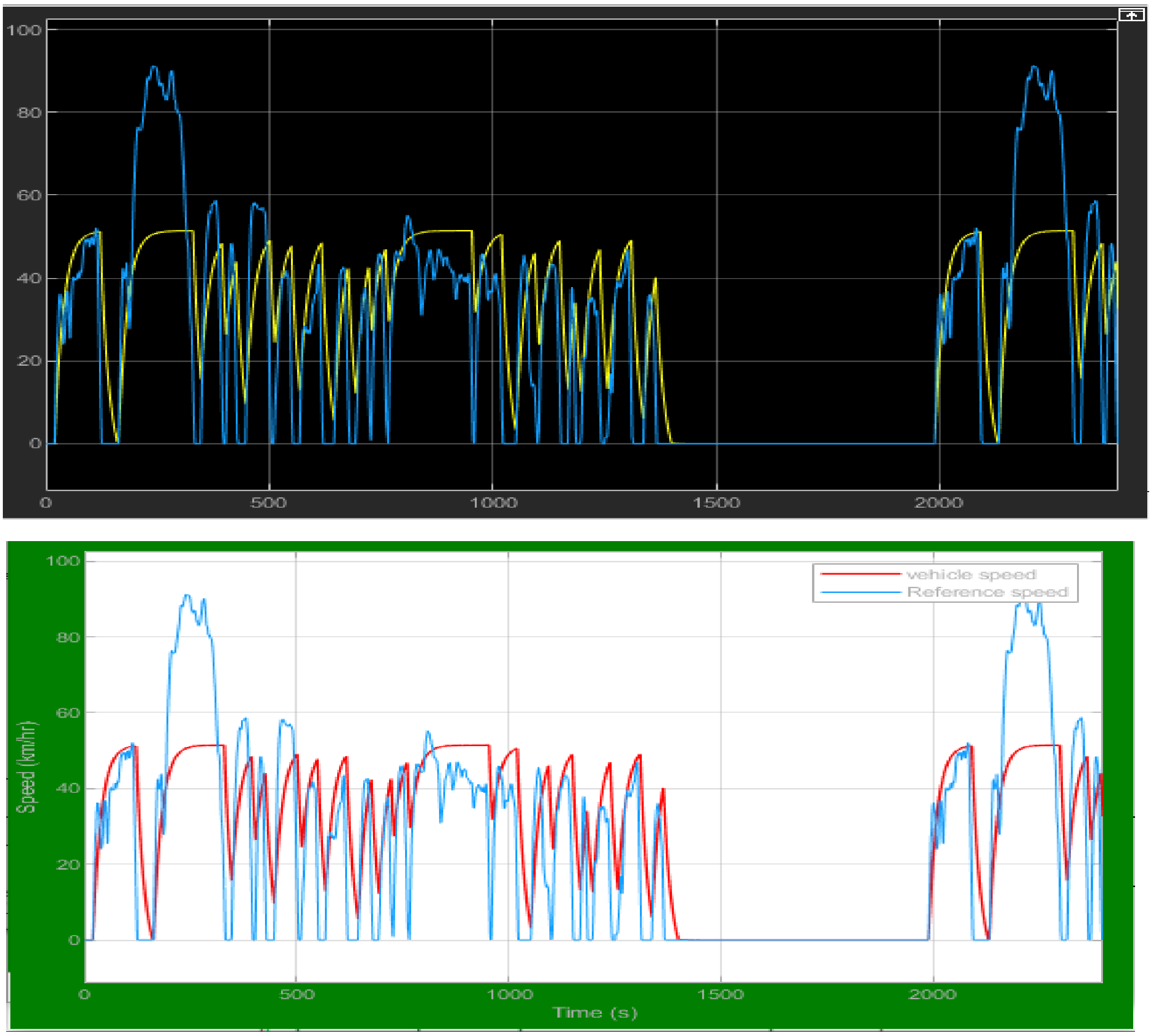

Figure 4. 4: vehicle speed analysis

The simulation curves for transient cycles, which are depicted in the aforementioned Figures, reveal that the drive cycle speed and vehicle speed almost completely overlap. It follows that for the selected motor and the specified specifications, the vehicle speed and the drive cycle speed were nearly equal. There is a little difference between the drive cycle and vehicle speed at several spots along drive cycle curves. This is a result of the vehicle's inertia's motor. The maximum speed of the vehicle is around 18.56 m/s (66.84 km/h), which is roughly identical to the reference velocity of the vehicle (blue curve) and the actual velocity of the vehicle (yellow or red curve). The inertial effect and associated control parameter are to blame for this slight variation.

4.2.2. Analysis of Range Covered by Vehicle

For fully charged battery and drive vehicle at 65 km/h with FTP75 drive cycle for 2474 sec. the distance travelled is around 66.56 km for 34% of battery usage and for fully used battery about 195 km was covered.

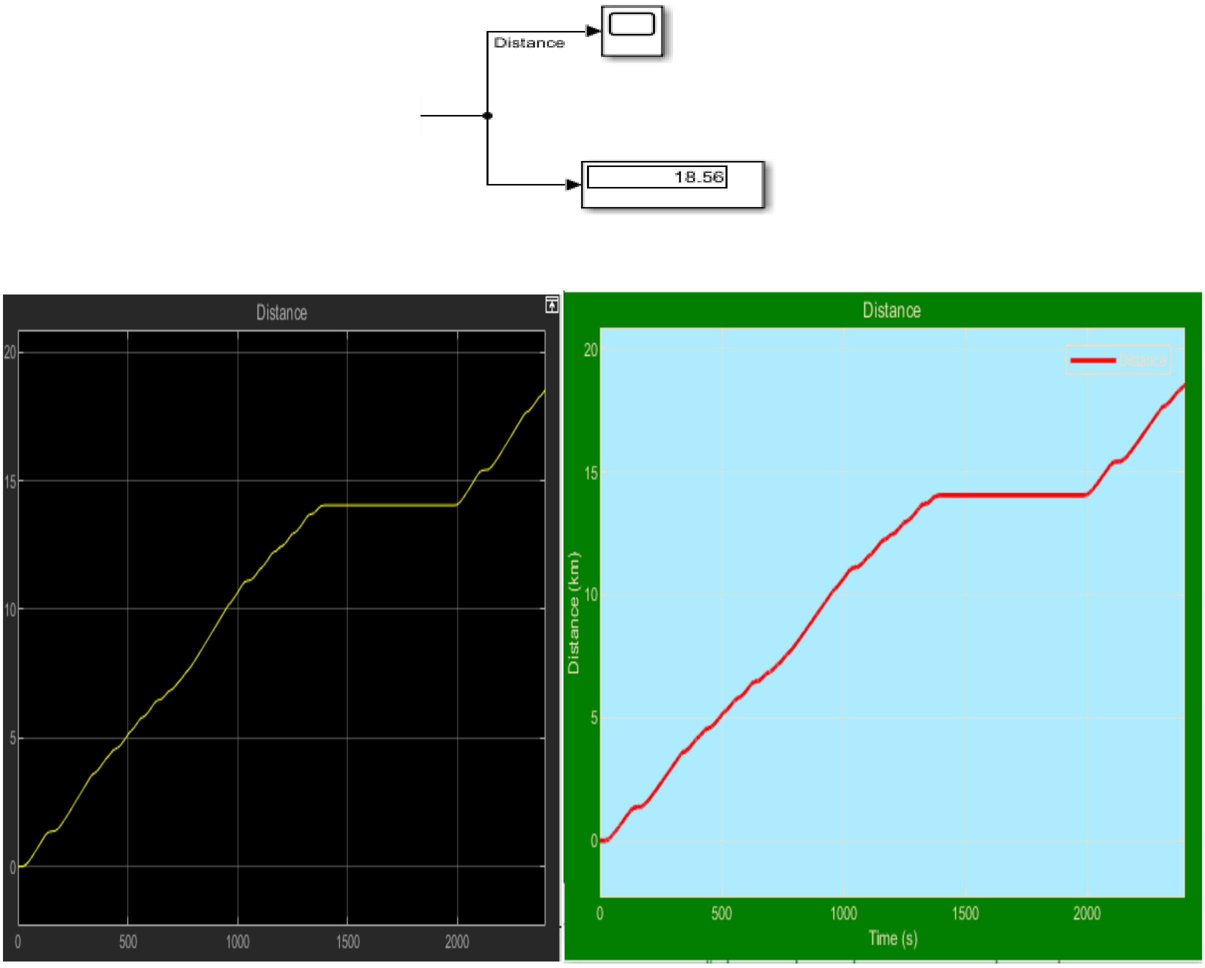

Figure 4. 5: Range covered by the vehicle

4.2.3. SOC Result Analysis

The SOC can be studied as follows based on the simulation of a Li-Ion battery with the provided drive cycle. The battery loses 34% SOC after travelling for 66.5 km and 2400 seconds, however it still maintains a SOC of 66% as shown in Figure 4.6 below. As shown in figure 4.6 below, the battery loses voltage when being accelerated. In contrast, when the car slows down, regenerative braking charges the battery.

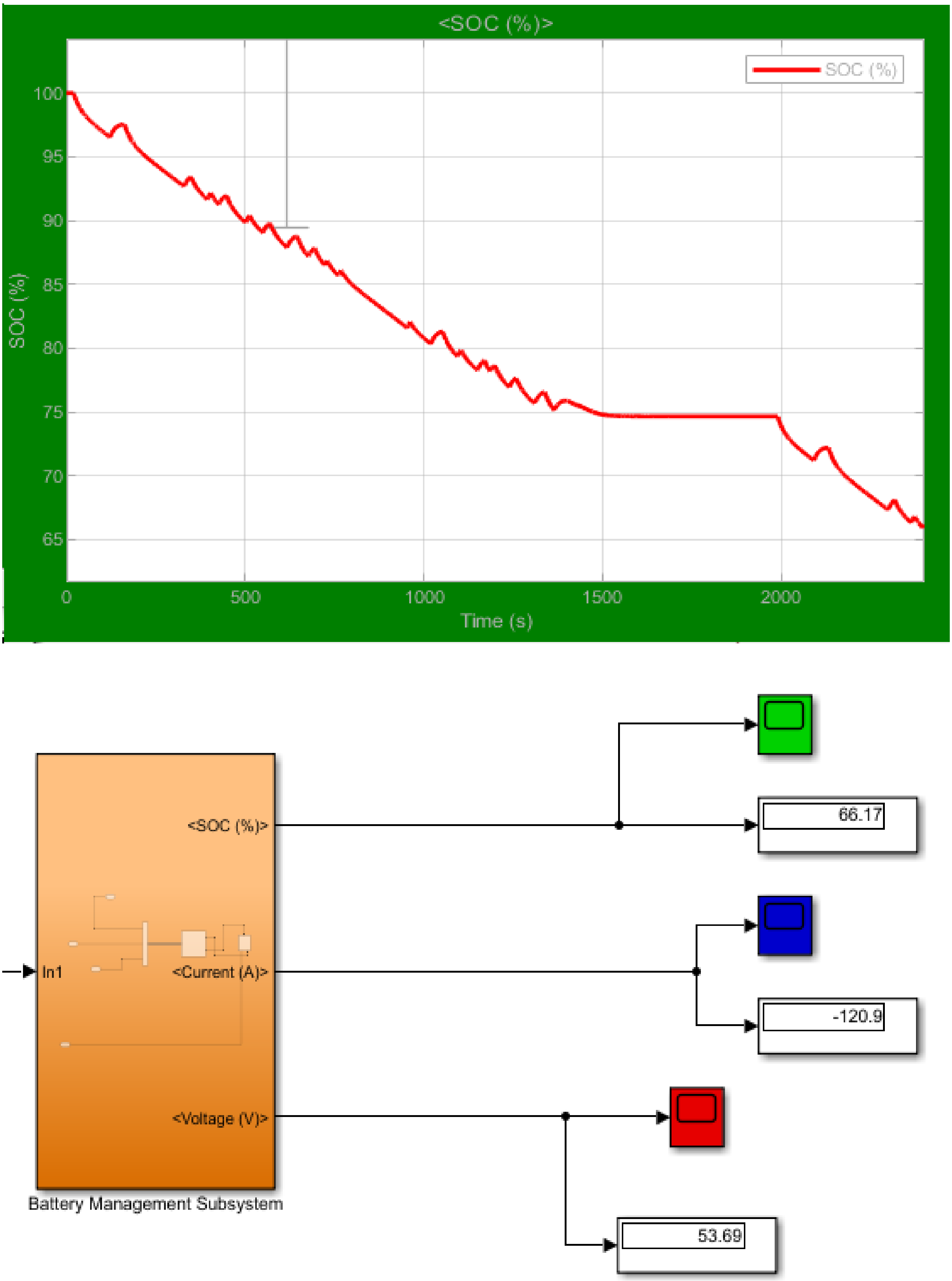

Figure 4. 6: Analysis of battery SOC

4.3. Battery Current

The battery current ranges from positive to negative values, as shown in Figure 4.7. The battery is being charged through regenerative braking when the current is negative, as opposed to the positive figure that indicates spent current.

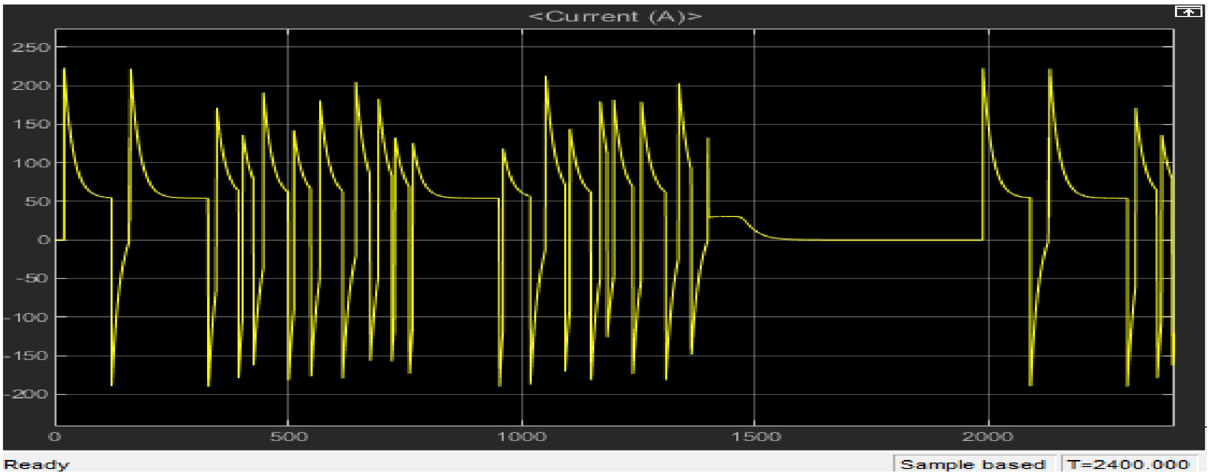

Figure 4. 7: Battery Current

4.4. Battery Voltage

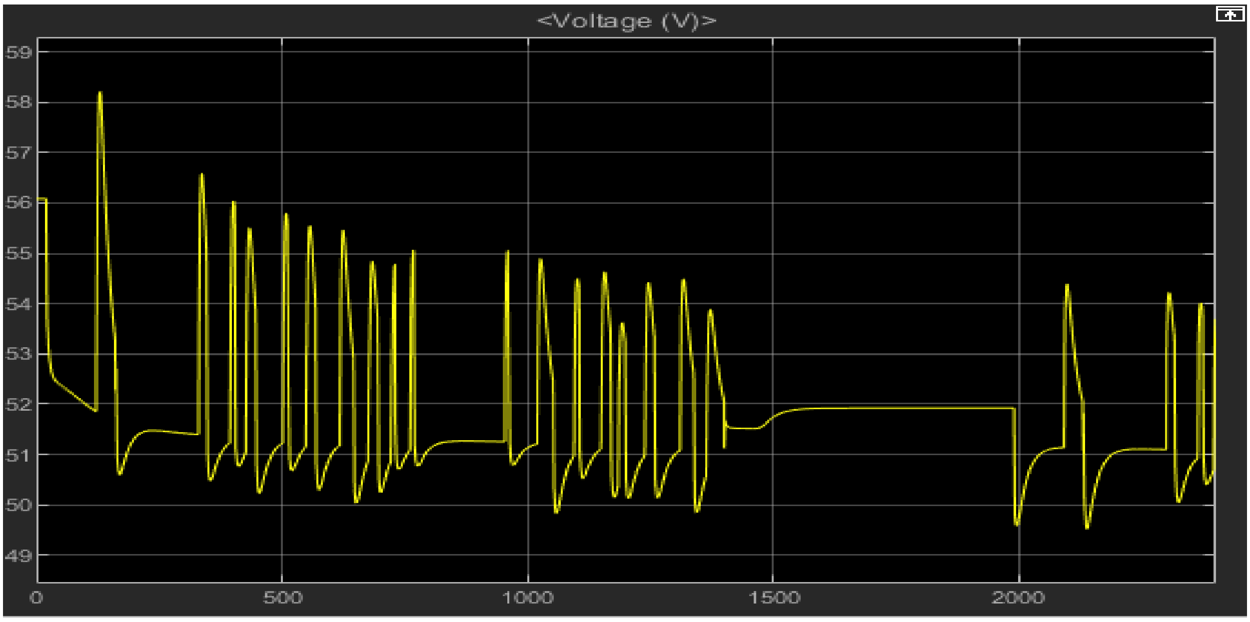

Figure 4. 8: Battery Voltage

4.5. Overall Vehicle Model

The general analysis made in this thesis was revealed that the obtained results in all analysis are validating the objective of modelling and simulation. The studies done before on this area with different researchers shows that the performance and range covered by electric vehicle depends on modelling of each and every components.

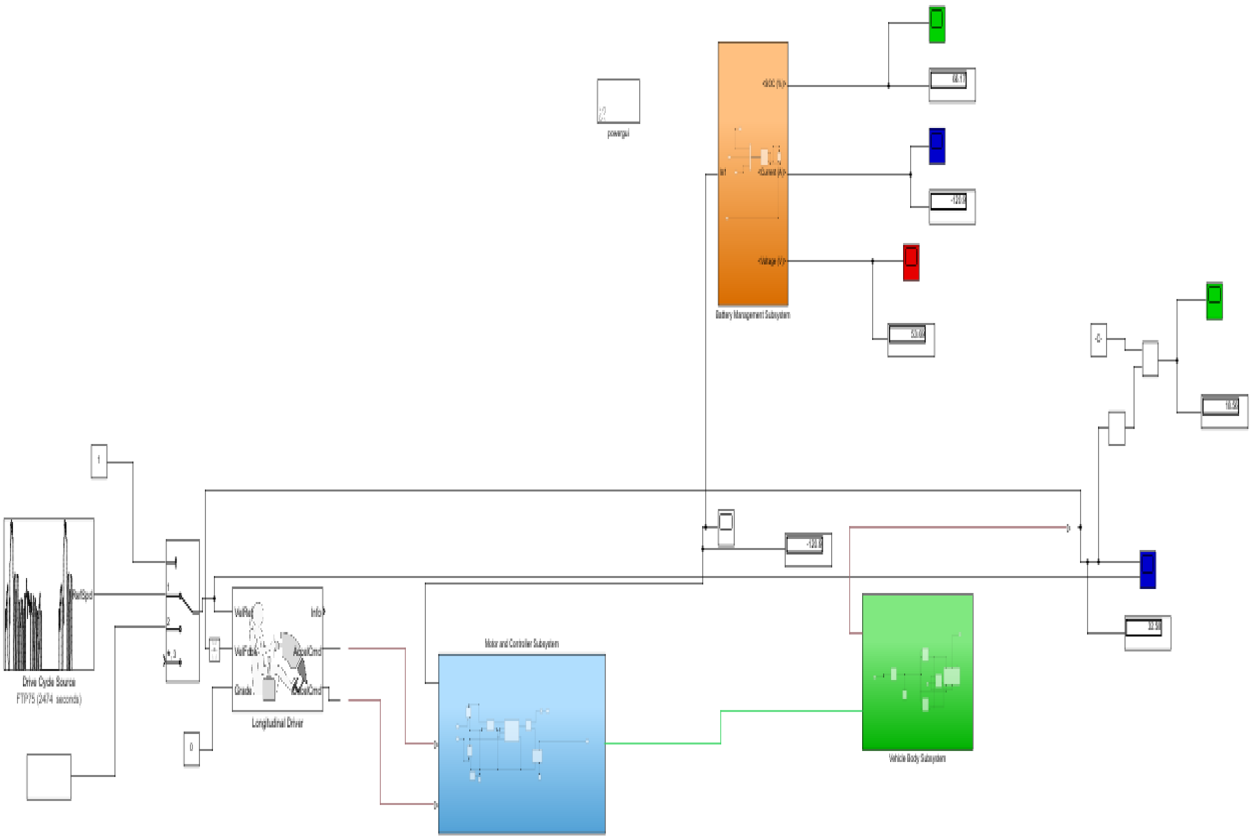

Figure 4. 9: Overall modelling of the vehicle

CHAPTER FIVE

CONCLUSION, SUMMARY, AND RECOMMENDATION

5.1. Summary

This summary provides a brief and concise account of the entire work of this thesis paper, as well as the objectives of the thesis up to the objective that was attained in this thesis work. The thesis's entitled, "Modelling and Simulation of three-wheeler Electric Vehicle Propelled by Permanent Magnet DC Motor" was initially chosen in response to the current global demand for electric vehicles.

Due to the size of the project and the necessity for additional study, I am now only designing the chassis portion of the three wheeler electric vehicle and conducting the analysis using the SOLIDWORKS and ANSYS software. A comprehensive model of the battery pack and the overall model of the vehicle's powertrain components were created in the MATLAB/Simulink environment to demonstrate how the entire three-wheeled electric vehicle functions. The motor and drive parameters were selected to closely resemble the three-wheeled electric vehicle system.

The physical modelling of Simscape was used to model all the parts of the powertrain. After the vehicle was designed and modelled, a longitudinal driver was added to test the vehicle's performance during acceleration and deceleration by comparing the drive cycle reference speed's command with the actual speed of the vehicle.

The results were very good in terms of displaying the battery's current and voltage as well as how the car moved throughout the drive cycle. The distance travelled in relation to the amount of battery charge used can then be assessed and simulated to display the battery's state of charge's (SOC) mileage for a specific range. This method can be utilised very efficiently in a variety of applications, including extending battery life.

5.2 Conclusion

Internal combustion engine-powered vehicles have been the technological advancement that has dominated the automobile industry and defined how global transportation systems have been set up. However, alternative engine technologies are already acquiring economic benefits, and businesses must adapt given the pressing need to decarbonize the global economy. Significant investments are made in hybrid and all-electric powertrains, as well as in innovative mobility ideas and services that operate at the nexus of the energy and transportation systems. How quickly they become competitive, which alternatives develop, and how quickly industries respond. The introduction to electric vehicles was addressed in this study together with historical developments up to the present. The loads operating on the vehicle chassis frame and the results of modal and harmonic analysis can also be found in adequate detail.

The model developed in this study is very easy to comprehend and provides a clear understanding of the many components used in electric vehicle modelling. Observations made from simulations of driving cycles show that the battery's state of charge and the distance travelled are influenced by the speed, acceleration, deceleration, and slope to which the vehicle is subjected. The simulation result done shows that the battery loses 34% SOC after travelling for 66.5 km and for 2400 seconds, however it still maintains a SOC of 66%. But, if the fully charged battery is used the range covered for single charged battery was about 195 km.

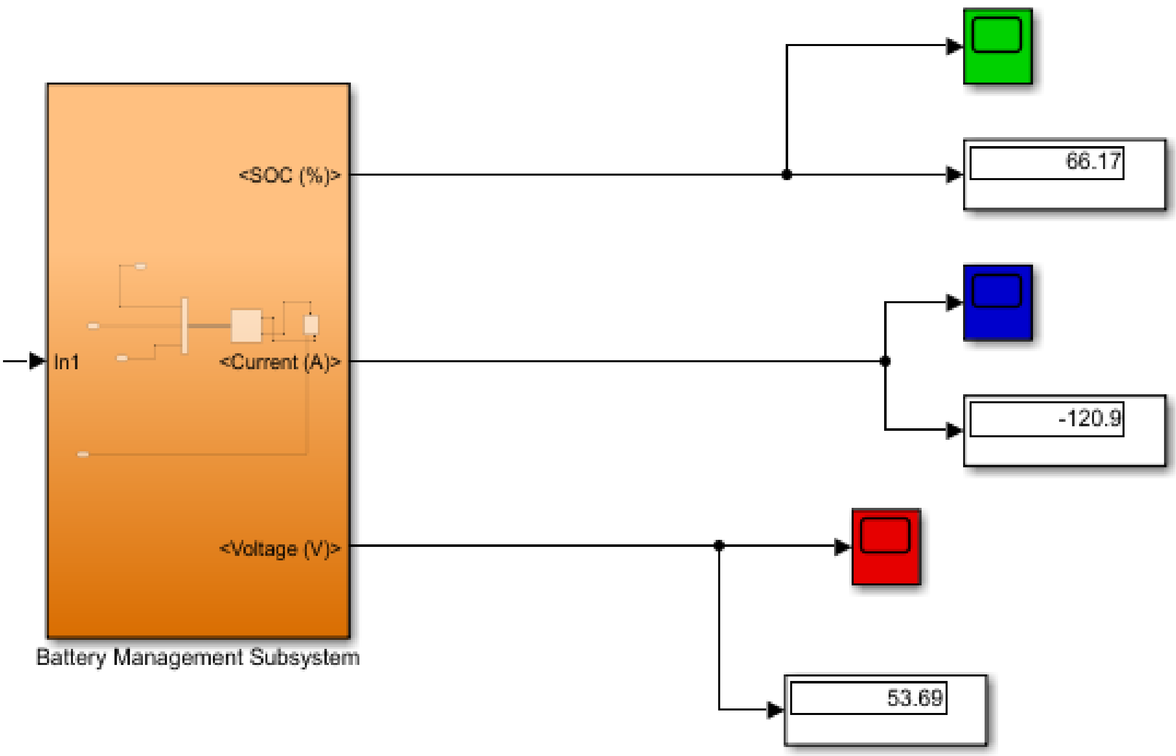

Figure 5. 1: Battery SOC

In real-world situations, an EV's range is influenced by the driving conditions in addition to its underlying technology. Due to the ongoing need for acceleration, 'stop and go' driving cycles use more energy than motorway driving cycles. Additionally, energy consumption increases with acceleration speed. Similar to how driving uphill is more energy-intensive than driving downhill or on flat terrain (Wai CK et.al, 2015). The ambient temperature also has an impact on energy consumption since it affects the utilisation of auxiliary devices and output energy losses (Morikawa T. et. al., 2018). Rolling resistance, aerodynamic drag, battery chemistry, and energy density all affect how far an electric vehicle can go (Sankaran G .et.al, 2020)

5.3 Recommendations

There are several places that can be improved upon in order to make this model even better. One significant area where this model might be improved significantly is by performing more optimisation to capture the regenerative braking energy. The battery, the body, the dc-dc converter, and the inverter analysis are some areas that should be improved to be more realistic. These elements were outside the purview of this project and add numerous non-linear effects.

These models can be used, though, to provide more precise findings for the energy optimisation. Although the actual parts (inductors, power MOSFETs, IGBTs, etc.) used to realise these subsystems can complicate modelling and simulation, they can also reveal new information about how the simulation as a whole behaves. This model can potentially be investigated further using various power supplies and energy storage systems, including fuel cells, ultra-capacitors, and others.

Further research might also done include thermal modelling for batteries that takes into account the impact of the surrounding temperature. With some familiarity with Matlab, Simscape, and other software programmes, this model is adaptable and simple to change. The manufacturer's specification documents can be used as a starting point for changing data inputs.

5.4 Future Work

Induction and DC motor drives, an H-bridge, and a PID controller are used in the majority of battery-powered vehicle manufacturers, including rickshaw companies, to create electric vehicles. Therefore, my future work will be a battery electric car with regenerative braking test, as well as the design of an entire three-wheel electric vehicle with a prototype that specifically focuses on solving the problem for disabled peoples with the use of such vehicles. Finally, I would like to offer anybody who want to conduct research on three wheeler electric vehicle as they do on this area.

REFERENCES

A. A. Bature, et al. (2001). Parameter Identification of a DC Motor. *IEEE International Conf. on Elec. Circuit and Systems*, 981-984.

A. A. R,. (2013). Control of Three Phase BLDC Motor using Fuzzy Logic Controller. *International Journal of Engineering Research & Technology (IJERT), Vols. 2*, 7.

Abd-Elhamid, A. S. (1680-1688). Cascade Control System of Direct Current Motor. *World Applied Sciences Journal*, 2012.

Abulifa, A. A., et al. (2017). Modelling and Simulation of battery Electric Vehicle by using MATLAB Simulink. *In Proc. IEEE 15th Student Conference on Research and Development* (pp. 383-387). New York: IEEE.

Amol Badgujar and P. A. Wankhade,. (2018). Static Analysis of Chassis Frame of Electric Tricycle. *International Journal of Scientific and Engineering Research Volume 9,Issue 5*, 2229-5518.

Ashish Kumar Singhal et al. (2015). Solar Electric Powered Hybrid Vehicle. *Journal of Electronic Design Technology Volume 6, Issue 3*, 2229-6980.

Atul Kumar and Dr. Prerna Gaur. (2014). Bidirectional DC/DC Converter for Hybrid Electric Vehicle. *IEEE Transactions on Advances in Computing, Communications and Informatics (ICACCI)*, 839-843.

Benjamin.C. (2011). *Investigation of DC motors for electric and hybrid electric motor vehicle.* Provo: BYU Scholars Archive.

Berjoza, D. & Jurgena,. (2017). “Influence of Batteries weight on Electric automobile performance”. *In Proc. Engineering for Rural Development* (pp. 1388-1394). Jelgava,Latvia: Latvia University of Agriculture.

Bhajana, V. V., and Pavel Drabek. (2015). A novel ZCS bidirectional buck-boost DC-DC converters for energy storage applications,. *Industrial Technology (ICIT), International Conference on IEEE,.* Thailand.

Bhatta, P. et al. (2019). Electrical Motors for Electric Vehicle –A Comparative Study. *In Proc. International Conference on “Recent Advances in Interdisciplinary Trends in Engineering & Applications* (p. 10). Amsterdam,Netherland: SSRN-ELSEVIER.

Castagnel, J. N. (1993). A Flexible Microcontroller Based Chopper Driving a Permanent Magnet DC Motor. *The European Power Electronics Application.*

Cheng He, et al. (2016). Design and Control of Switched Reluctance Motor Drive for Electric Vehicles. *14th International Conference on Control, Automation, Robotics & Vision Phuket* (pp. 54-65). Thailand: ICARCV.

D. van Niekerk and D.V. Nicolae. (2015). Brushless Direct Current Motor EfficiencyCharacterization. *IEEE*, 978-1-4763.

Daziano, R. A., & Chiew, E. (2013). On the effect of the prior of bayes estimators of the willingness to pay for electric-vehicle driving range. *Transportation Research Part D:, 21*(10), 7-13.

Ehsani, M. et al. (2005). *Modern Electric, Hybrid Electric,and Fuel Cell Vehicles.* Filorida: CRC Press.

G. Ren, et al. (2015). Review of electrical energy storage system for vehicular applications. *Renewable and Sustainable Energy Reviews*, 225-236.

George, M. (2008). Speed Control of Separately Excited DC Motor. *American Journal of Applied Sciences 5 (3)*, 227-233.

Gupta Gaurav and Prerna Gaur. (2015). Fuzzy logic controlled-power factor corrected bridgeless buck boost converter-fed brushless DC motor drive. *Computer, Communication and Control (IC4), International Conference on. IEEE.* Thailand: IEEE press.

Gupta, V. (2010). Working and Analysis of the H – Bridge Motor Driver Circuit Designed for Wheeled Mobile Robots. *Advanced Computer Control (ICACC)*, (pp. 27-29). Shenyang, China.

Hua J. and Ouyang M. (2012). A review on the key issues for lithium-ion battery management in electric vehicles,. *Journal of Power Sources,*, 272-288.

Hughes, A. (2006). *Electric Motors and Drives Fundamentals, Types and Applications.* Austin Hughes: Elsevier Ltd.

J. Ruderman, et al. (2008). Optimal State Space Control of DC Motor. *Proceedings of the 17th World Congress of the International Federation of Automatic Control*, (pp. 5796-5801). Seoul, Korea.

J. Santana, et al. (2002). Simulation and Construction of Speed Control for DC Series Motor. In J. L. J. Santana, *Mechatronics, Vol.12(9)* (pp. 1145-1156). USA: Elsevier Science Ltd.

J.A.K.S.Jayasinghe,B.S. et. al. (2009). Aerodynamic Drag and Rolling Resistance of Three Wheelers. *The Institution of Engineers,* 21- 29.

J.B.Gupta. (2015). *Theory & Performance of ELECTRICAL MACHINES.* S.K.Kataria& Sons.

J.Chapman, S. (2007). *Electric Machinery Fundamentals.* Hungary: McGraw-HILL.

Jayakaran, S. (2017). Design and Analysis of suspension system for a three wheeler electric vehicle. *Journal of Advanced Research in Dynamical and Control Systems*, 1230-1238.

Karthick, R. (2004). PC Based Speed Controlling of a DC Motor. *Report, Circuit Ideas, Electronics for you*, 67.

Kumar, K. M. (2017). A Bidirectional converter using fuzzy controller. *International Journal for Research in Applied Science & Engineering.Technology (IJRASET)*, vol 5.

Kusum, P. C. (2018). Design of Electric Vehicle. *International Journal of Advance Engineering Research,*, 25-37.

Leitman, S., & Brant, B. (2009). *Build your own Electric Vehicle.* New York,USA: McGraw Hill.

Leitman.S. (2010, Appril 1). *Electric Auto Association*. Retrieved from http://www.eaaev.org/History/index.html.: http://www.eaaev.org/History/index.html.

Lulhe, A. M. & Date, T. N. (2015). A Design & MATLAB Simulation of Motor Drive used for Electric Vehicle. *In Proc. International Conference on Control, Instrumentation,Communication and Computational Technologies* (pp. 739-743). Kumaracoil,India: IEEE.

Lulhe, A. M. (2015). A Technological review paper for drives used in electric vehicle (EV) and hybrid electric vehicles (HEV). *In Proc. International Conference on Control, Instrumentation, Communication and Computational Technologies,* (pp. 700-705). Kumaracoil,India: Los Alamitos,Calif.

M. Hannan, et al. (2017). Review of energy storage systems for electric vehicle applications. *Issues and challenges," Renewable and Sustainable Energy Reviews*, 771-789.

M. N. Kamarudin and S. M. Rozali. (2008). Simulink Implementation of Digital Cascade Control DC Motor Model. *Proc. IEEE 2nd International Power and Energy Conf. (PECon '08)* (pp. 1043-1048). Malaysia: IEEE.

M.V.Ramesh, et al. (2000). Speed Torque characteristics of Brushless DC motor in either direction on load using ARM controller. *IEEE Transactions on Industry Applications,*, 1-36.

Martins, F. et al. (2019). Analysis of Fossil Fuel Energy Consumption and Environmental Impacts in European Countries. *Energies*, 964.

Mohammed, J. A. (2013). PulseWidth Modulation for DC Motor Control Based on LM324. *Eng. &Tech. Journal, Vol. 31,Part (A), No.10*, 1882-1896.

Morikawa T .et.al. (2018). Exploring the interactive effects of ambient temperature and vehicle auxiliary loads on electric vehicle energy consumption. *Appl Energy*, 324-331.

Negash, p. M. (2017). *Fuzzy logic control based bidirectional power low capability between the electric vehicle and dc or ac grid,.* Telangana.

Ovidiu, B. (2012). Energy Management of Electric and Hybrid vehicles dependent on powertrain configuration. *Central European Journal of Engineering*, 253-263.

Parag Kulkarni. (2015). Review of Hybrid Electrical Vehicles. *International Journal of Emerging Research in Management &Technology Volume-4, Issue-3*, 2278-9359.

Patel, S. (2016). Design And Development Of Three Wheeled Campus Vehicle. *International Journal Of Scientific & Technology Research Volume 5, Issue 08,, 5*(08), 2277-8616.

Porselvi, T., et al. (2017). Selection of Power Rating of an Electric Motor for Electric Vehicles. *International Journal of Engineering and Computing,* 6469-6472.

R. Bullock. (2001). *Applying PMDC motors.* Retrieved from Bison Gear & Engineering Corp: http://machinedesign.com/motorsdrives/applying-pmdc-motors

Rashid, M. H. (2004). *Power Electronics, Devices, and Applications.* NJ, USA: Pearson Prentice Hall.

RuiEstevesAraújo, et al. (2005). A Low Cost Induction Motor Controller for Light Electric Vehicles in Local Areas. *IEEE ISIE*, 20-23.

S Devi Vidhya and M Balaji. (2019). Modelling, Design and Control of a Light Electric Vehicle with Hybrid Energy Storage System for Indian Driving Cycle. *Measurement and Control*, 1420-1433.

S. Manzetti and F. Mariasiu. (2015). Electric vehicle battery technologies: From present state to future systems. *Renewable and Sustainable Energy Reviews*, 1004-1012.

S.M.Baque Billah and K.K.Islam. (2016). Regenerative Braking Characteristics of PMDC Motor by Applying Different Armature Voltage. *International Conference on Electrical, Computer and Telecomminication Engineering* (pp. 1-5). Gazipur, Bangladesh: IEEE.

S.M.H.S. Omar et al. (2015). Design And Optimization Of Powertrain System For Prototype Fuel Cell Electric Vehicle. *Journal Of Mechanical Engineering And Sciences (Jmes) Volume 8*, 2289-4659.

Sankaran G .et.al. (2020). Range anxiety on electric vehiclesin India- Impact on customer and factors influencing range anxiety. *Materials Today Proc.* (pp. 895-901). Tamil Nadu: Elsevier B.V.

Satinder.S and Beant .S. (2014). Design optimization and statical crash analysis of chassis frame for off road vehicle. *International Journal of Automobile Engineering Research and Development*, 2277- 4785.

Sharada Prasad N & K R Nataraj. (2014). "Design And Development Of Hybrid Electric Twowheeler Suitable For Indian Road Conditions",. *International Journal Of Electrical, Electronics And Data Communication Volume-2, Issue-9*, 2320-2084.

Singh, N. (2017). Dynamic Analysis and Shape Optimization of Electric Car Chassis. *International Journal of Aerospace and Mechanical Engineering, Volume 4*, 2393-8609.

Sinha, R., and Bangia, S. (2021). Performance Analysis of Electric Vehicle Based on Various Working Scenarios. *International Transaction Journal of Engineering, Management, & Applied Sciences & Technologies*, *12*(1), 1-15.

Sreejith R. et. al. (2016). Modelling and analysis of PMBLDC motor based three wheeler EV for closed loop optimum operation. *Power electronics drives and energy systems* (pp. 1-5). Trivandrum,India: IEEE.

Sreejith R. et.al. (2016). Modelling and Analysis of PMBLDC motor based three wheeler EV for closed loop optimum operation. *Power electronics drives and energy systems* (pp. 1-5). Trivandrum, India: IEEE.

Sudhansu, S. a. (2022). Modeling designing and controlling a three wheeled electric vehicle and implemented in hardware. *Research article,* 1-12.

Tendillo, L. A. (2015). *Design and control of a bidirectional dc/dc converter for an electric vehicle application.* Tarragona.

The history of alternative fuels in transportation, 01103559 (Utilities Policy June 2, 2008).

Wai CK et.al. (2015). Simulation of a Distance estimator for battery electric vehicle. *Alexandria Eng*, 359-371.

Warake, K. et al. (2018). "Design & Development of Regenerative Braking System at Rear Axle". *International Journal of Advanced Mechanical Engineering*, 165-172.

Wikipedia contributors,. (2020, 4 19). *Wikipedia*. Retrieved from The Free Encyclopedia.: http://www.wikipedia.com

Wu,Licheng, et al. (2011). A non-Tethered Telecontrollable Water Strider Robot. *International Journal of Advanced Robot*, 5772/45704.

X. D. Xue and N.C Cheung. (2008). Selection of Electric Motor Drives for Electric Vehicles,. *Australasian Universities Power Engineering Conference (AUPEC'08).* Australia.

Xin. X., et al. (2020). A novel State of Charge estimation method for ternary Lithium Batteries based on system function and extended Kalman Filter. *International Journal of Electrochemical Science,*, 2226-2242.

Yildiz, A. B. (2012). Electrical equivalent circuit based modeling and analysis of direct current motors. *International Journal of Electrical Power & Energy Systems*, 1043-1047.

APPENDIX A

SolidWorks Modelling and Ansys Analysis of Three Wheeler Electric Vehicle

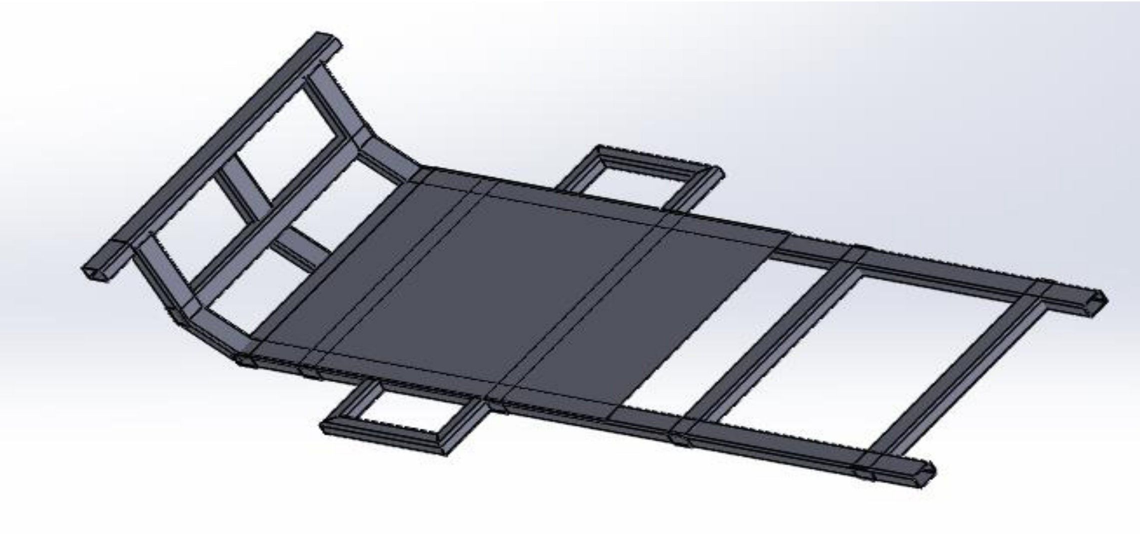

Figure A. 1: 3D modelling of three wheeler electric vehicle chassis

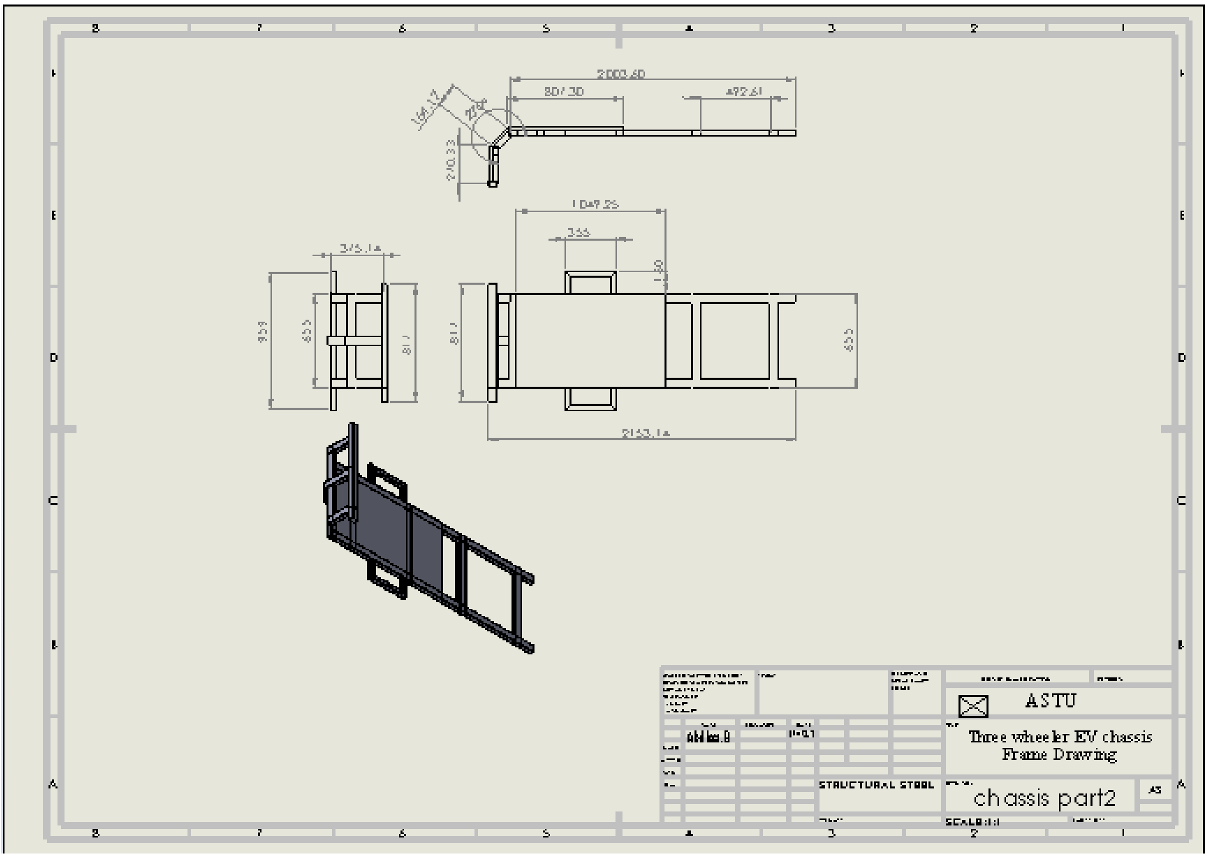

Figure A. 2: Detailed Drawing of three wheeler electric vehicle chassis

ANSYS Analysis of Three Wheeler Electric Vehicle Chassis Frame

Author	Abdissa Regassa
Subject	MSc Thesis
Prepared for	Three Wheeler Electric Vehicle Chassis Analysis
First Saved	Sunday, April 2, 2023
Last Saved	Sunday, April 2, 2023
Product Version	16.0 Release
Save Project Before Solution	Yes
Save Project After Solution	Yes

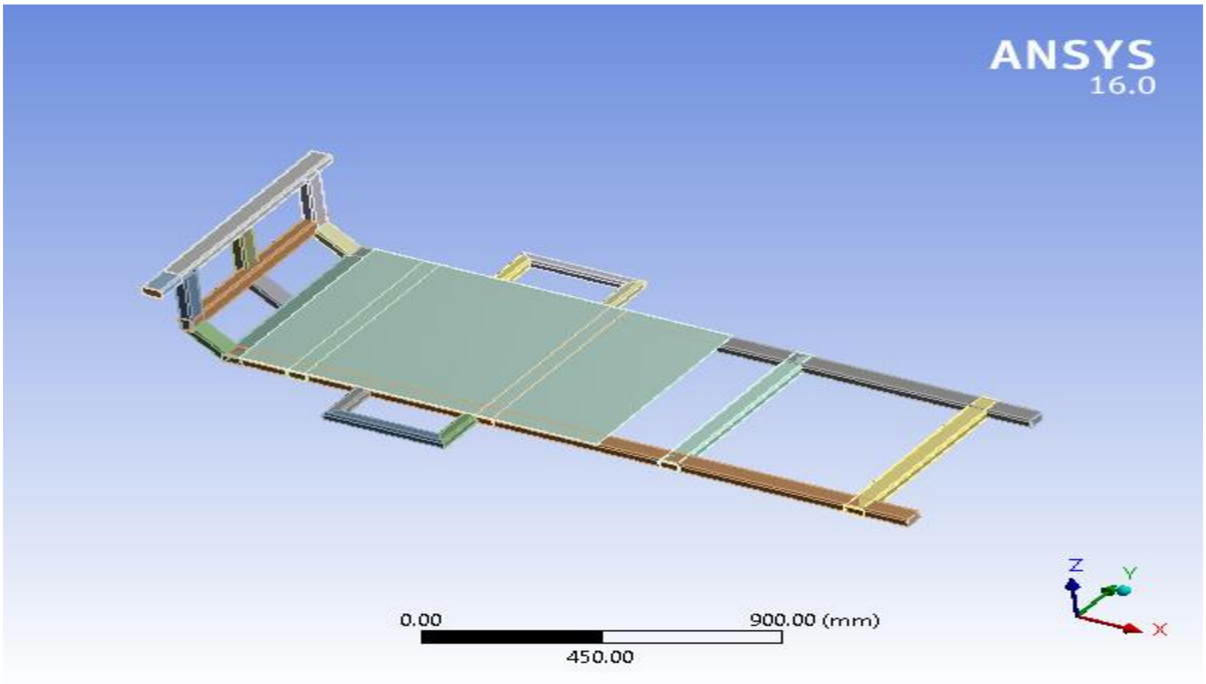

Table A. 1: Model Properties and Results

1. Units

Unit System	Metric (mm, kg, N, s, mV, mA) Degrees rad/s Celsius
Angle	Degrees
Rotational Velocity	rad/s
Temperature	Celsius

2. Mesh

Object Name	Mesh
State	Solved
Display	
Display Style	Body Color
Defaults	
Physics Preference	Mechanical
Relevance	0
Sizing	
Use Advanced Size Function	Off
Relevance Center	Fine
Element Size	Default
Initial Size Seed	Active Assembly
Smoothing	Medium
Transition	Fast
Span Angle Center	Fine
Minimum Edge Length	2.0 mm
Inflation	
Use Automatic Inflation	None
Inflation Option	Smooth Transition
Transition Ratio	0.272
Maximum Layers	5
Growth Rate	1.2
Inflation Algorithm	Pre
View Advanced Options	No
Patch Conforming Options	
Triangle Surface Mesher	Program Controlled
Patch Independent Options	
Topology Checking	No
Advanced	
Number of CPUs for Parallel Part Meshing	Program Controlled
Shape Checking	Standard Mechanical
Element Midside Nodes	Program Controlled
Straight Sided Elements	No
Number of Retries	Default (4)
Extra Retries For Assembly	Yes
Rigid Body Behavior	Dimensionally Reduced
Mesh Morphing	Disabled
Defeaturing	
Pinch Tolerance	Please Define
Generate Pinch on Refresh	No
Automatic Mesh Based Defeaturing	On
Defeaturing Tolerance	Default
Statistics	

Nodes	165120
Elements	27925
Mesh Metric	None

3. Modal Analysis

Object Name	Modal (A5)
State	Solved
Definition	
Physics Type	Structural
Analysis Type	Modal
Solver Target	Mechanical APDL
Options	
Environment Temperature	22. °C
Generate Input Only	No
Object Name	Pre-Stress (None)
State	Fully Defined
Definition	
Pre-Stress Environment	None
Object Name	Analysis Settings
State	Fully Defined
Options	
Max Modes to Find	6
Limit Search to Range	No
Solver Controls	
Damped	No
Solver Type	Program Controlled
Rotordynamics Controls	
Coriolis Effect	Off
Campbell Diagram	Off
Output Controls	

Stress	Yes
Strain	Yes
Nodal Forces	No
Calculate Reactions	Yes
Store Modal Results	Program Controlled
General Miscellaneous	No
Analysis Data Management	
Solver Files Directory	C:\Users\ma\Documents\modal analysis trial_files\Modal ad Harmonic Analysis_files\dp0\SYS\MECH\
Future Analysis	MSUP Analyses
Scratch Solver Files Directory	
Save MAPDL db	Yes
Delete Unneeded Files	Yes
Solver Units	Active System
Solver Unit System	Nmm
Object Name	Fixed Support
State	Fully Defined
Scope	
Scoping Method	Geometry Selection
Geometry	13 Faces
Definition	
Type	Fixed Support
Suppressed	No

3.1. Solution

Mode	Frequency [Hz]
1.	17.574
2.	22.79
3.	25.839
4.	39.748
5.	51.723
6.	68.58

Object Name	Total Deformation	Total Deformation 2	Total Deformation 3	Total Deformation 4	Total Deformation 5	Total Deformation 6
State	Solved					
Scope						
Scoping Method	Geometry Selection					
Geometry	All Bodies					
Definition						
Type	Total Deformation					
Mode	1.	2.	3.	4.	5.	6.
Identifier						
Suppressed	No					
Results						
Minimum	0. mm					
Maximum	17.437 mm	26.175 mm	28.599 mm	5.4635 mm	60.764 mm	33.231 mm
Minimum Occurs On	Part 15					
Maximum Occurs On	Part 3				Part 5	Part 14
Information						
Frequency	17.574 Hz	22.79 Hz	25.839 Hz	39.748 Hz	51.723 Hz	68.58 Z

4. Harmonic Response Analysis

Object Name	Harmonic Response (B5)
State	Solved
Definition	
Physics Type	Structural
Analysis Type	Harmonic Response
Solver Target	Mechanical APDL
Options	
Environment Temperature	22. °C
Generate Input Only	No

Object Name	Analysis Settings
State	Fully Defined
Options	
Frequency Spacing	Linear
Range Minimum	0. Hz
Range Maximum	68.58 Hz
Solution Intervals	10
Solution Method	Mode Superposition
Include Residual Vector	No
Cluster Results	No
Store Results At All Frequencies	Yes
Rotordynamics Controls	
Coriolis Effect	Off
Output Controls	
Stress	Yes
Strain	Yes
Nodal Forces	No
Calculate Reactions	Yes
Expand Results From	Program Controlled
-- Expansion	Modal Solution
General Miscellaneous	No
Damping Controls	
Constant Damping Ratio	0.
Stiffness Coefficient Define By	Direct Input
Stiffness Coefficient	0.
Mass Coefficient	0.
Save MAPDL db	No
Delete Unneeded Files	Yes

Solver Units	Active System
Solver Unit System	Nmm

4.1. Solution

Object Name	Frequency Response	Frequency Response 2
State	Solved	
Scope		
Scoping Method	Geometry Selection	
Geometry	24 Bodies	
Spatial Resolution	Use Average	
Definition		
Type	Directional Deformation	
Orientation	X Axis	
Suppressed	No	
Options		
Frequency Range	Use Parent	
Minimum Frequency	0. Hz	
Maximum Frequency	68.58 Hz	
Display	Bode	
Chart Viewing Style	Log Y	
Results		
Maximum Amplitude	3.516e-002 mm	
Frequency	20.574 Hz	
Phase Angle	0. °	
Real	3.516e-002 mm	
Imaginary	0. mm	

5. Material

5.1. Structural Steel

Density	7.85e-006 kg mm^-3
Coefficient of Thermal Expansion	1.2e-005 C^-1
Specific Heat	4.34e+005 mJ kg^-1 C^-1
Thermal Conductivity	6.05e-002 W mm^-1 C^-1
Resistivity	1.7e-004 ohm mm

APPEDIX B

Matlab-Simulink Modelling of Three Wheeler Electric vehicle

Table B. 1: Specification of Three Wheeler Electric Vehicle

No	Parameter	Symbol	Value
1	Vehicle mass	M	700 Kg
2	Maximum Power	P	7.25 Kw
3	Wheel base	B	1318 mm
4	Overall length	L	2635 mm
5	Overall width	W	1300 mm
6	Overall height	H	1710 mm
7	Coefficient of rolling friction	C_{rr}	0.015
8	Frontal area	A	0.35 m^2
9	Aerodynamic drag coefficient	C_d	0.2
10	Tyre	R	4.0 * 8.0
11	Maximum speed	N	65 Km/hr
12	Grade angle	ϴ	6^0

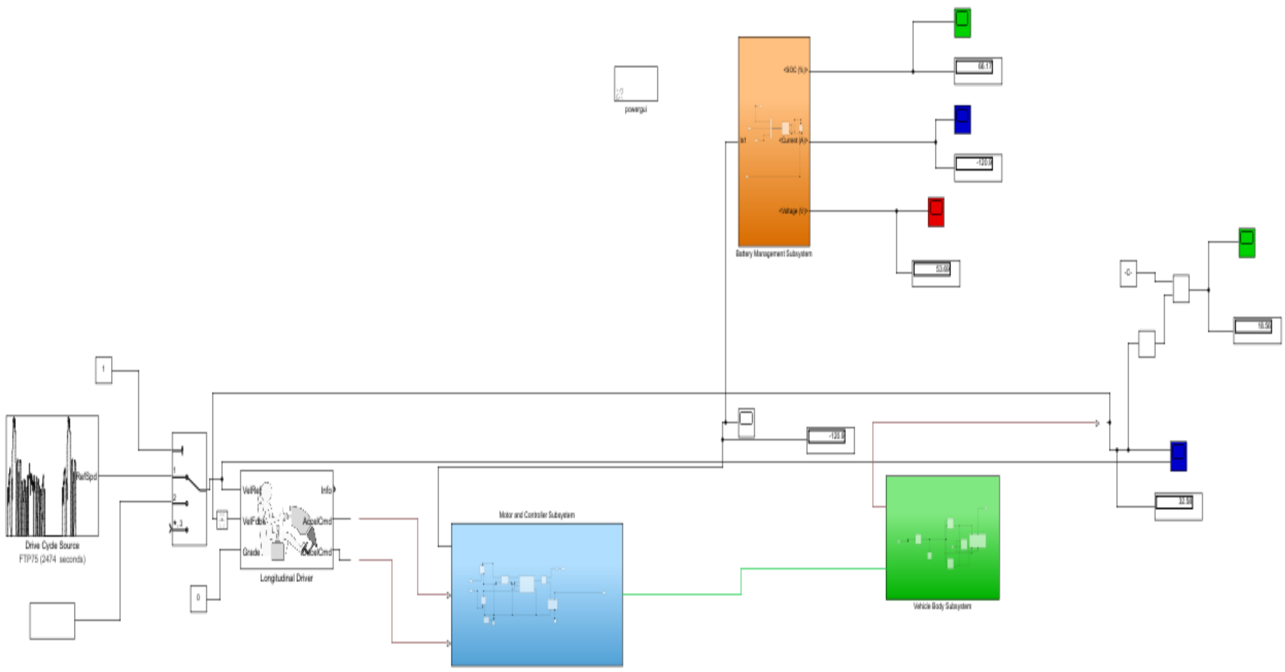

Figure B. 1: Overall Modelling of Three Wheeler Electric Vehicle